Robust Realized Integrated Beta Estimator with Application to Dynamic Analysis of Integrated Beta

Minseog Oh[a], Donggyu Kim[a], and Yazhen Wang[b]

[a]Korea Advanced Institute of Science and Technology (KAIST),

[b]University of Wisconsin-Madison

December 13, 2023

Abstract

In this paper, we develop a robust non-parametric realized integrated beta estimator using high-frequency financial data contaminated by microstructure noise, which is robust to the stylized features, such as the time-varying beta and the price-dependent and autocorrelated microstructure noise. With this robust realized integrated beta estimator, we investigate dynamic structures of integrated betas and find a persistent autoregressive structure. To model this dynamic structure, we utilize the autoregressive-moving-average (ARMA) model for daily integrated market betas. We call this the dynamic realized beta (DR Beta). Then, we propose a quasi-likelihood procedure for estimating the parameters of the ARMA model with the robust realized integrated beta estimator as the proxy. We establish asymptotic theorems for the proposed estimator and conduct a simulation study to check the performance of finite samples of the estimator. The proposed DR Beta model with the robust realized beta estimator is also illustrated by using data from the E-mini S&P 500 index futures and the top 50 large trading volume stocks from the S&P 500 and an application to constructing market-neutral portfolios.

Key words and phrases: high-frequency financial data, pre-averaging estimation, quasi-maximum likelihood estimation, time-varying beta.

1 Introduction

Market beta is a statistical measure of assets' sensitivity to the overall market. This measure plays a central role as the systemic risk measurement in financial applications such as asset pricing, risk management, and portfolio allocation (Fama and French, 2004; Perold, 2004). Thus, the characteristic of the market beta is a primary concern in empirical finance. Especially, several empirical studies reported that market betas vary over time (Bos and Newbold, 1984; Breen et al., 1989; Hansen and Richard, 1987; Keim and Stambaugh, 1986). To account for the time-varying property, low- and high-frequency finance modeling approaches have been independently adopted. In the low-frequency financial modeling approach, we often employ discrete-time series regression models in either a non-parametric or parametric framework based on low-frequency data such as daily, weekly, and monthly return data. For example, Fama and MacBeth (1973) used a rolling window regression approach with the ordinary least square (OLS) method, and Black et al. (1992) employed the state-space model by using the Kalman filter method. In addition, to account for market beta dynamics, several studies proposed autoregressive time series models, such as generalized autoregressive conditional heteroskedasticity (GARCH) model-type structures (Engle, 2016; González-Rivera, 1996; Koutmos et al., 1994; Ng, 1991). In contrast, Bollerslev et al. (2016) showed that incorporating high-frequency financial data offers more benefits while capturing beta dynamics. Specifically, intraday data provide accurate estimations with sufficient data even within a short time period. To exploit this property, several non-parametric market beta estimators based on high-frequency data under continuous-time series regression models have been developed. For example, Barndorff-Nielsen and Shephard (2004) employed the OLS method by calculating a ratio of the integrated covariance between assets and systematic factors to the integrated variation of systematic factors. See also Andersen et al. (2006); Li et al. (2017a); Mykland and Zhang (2006); Reiß et al. (2015). Mykland and Zhang (2009) further

computed the market beta as the aggregation of market betas estimated over local blocks. Aït-Sahalia et al. (2020) proposed an integrated beta approach, using spot market betas in the absence of market microstructure noise, and Andersen et al. (2021) investigated intraday variation of spot market betas. Jacod and Rosenbaum (2013) introduced the non-parametric inference for nonlinear volatility functionals of general multivariate Itô semimartingales in a high-frequency, but without the presence of noise. Recently, Chen (2018) extended this non-parametric inference to contexts with the presence of microstructure noise. They do not allow for any dependent structure of the microstructure noise on the true latent price, nor do they account for its autocorrelation. However, several studies indicated that the microstructure noise is not only dependent on the true latent price but also exhibits autocorrelation (Hautsch and Podolskij, 2013; Jacod et al., 2019; Li et al., 2020; Li and Linton, 2022, 2023). Thus, to measure the market beta accurately, we need to develop a robust realized beta estimation procedure.

In this paper, to accommodate the stylized features, such as the time-varying beta and the price-dependent and autocorrelated microstructure noise, we develop a robust realized integrated beta (RIB) estimator for integrated betas with high-frequency data contaminated by price-dependent and autocorrelated microstructure noise. For example, to handle the time-varying spot beta process and the price-dependent and autocorrelated microstructure noise, we estimate spot volatilities using the robust pre-averaging method (Jacod et al., 2019). Then, we can calculate the spot betas using spot volatility estimators. However, due to the microstructure noise, they have asymptotically diverged bias with a convergence rate of $m^{-1/4}$, which is known as the optimal with the presence of microstructure noise. To overcome this problem, we introduce a bias adjustment scheme and integrate the bias-adjusted spot beta estimators to obtain the realized integrated beta estimator. We show its asymptotic properties and obtain the convergence rate $m^{-1/4}$. To the best of our knowledge, the proposed RIB is the first integrated beta estimator, which is robust to the financial features, such as the time-varying beta and the price-dependent and autocorrelated microstructure noise. Since the proposed RIB estimation procedure provides an accurate and robust market beta estimator, it may help us study the dynamic structures of integrated market betas.

With the RIB estimator, we find that the realized betas have persistent autoregressive (AR) structures (see Figure 1 in Section 3). This result coincides with the previous literature. The literature on beta dynamics predominantly employs two approaches; modeling conditional covariance (Engle, 2016; González-Rivera, 1996; Hansen et al., 2014; Koutmos et al., 1994; Ng, 1991) and directly modeling conditional beta. Adrian and Franzoni (2009); Ang and Chen (2007); Blume (1971) employed AR(1) structure to analyze beta dynamics based on low-frequency data, such as monthly or quarterly stock returns. Andersen et al. (2006); Becker et al. (2021); Hollstein and Prokopczuk (2016) employed the class of ARFIMA structure on monthly, quarterly, and semiannual beta, estimated from 30-minute and daily returns. In this paper, we model the daily integrated betas using the ARMA(p, q) model to capture the persistent AR structure and call this dynamic realized beta (DR Beta). To estimate the parameters of the ARMA model, we suggest a quasi-maximum likelihood estimation procedure with the robust non-parametric RIB estimator. For example, we use RIB as the proxy for the corresponding conditional expected integrated beta and employ the well-known least square loss function. It is crucial to use a consistent estimator when working with the ARMA model, as measurement errors can significantly jeopardize estimation and prediction accuracy (Koreisha and Fang, 1999). Since incorporating ultra-high-frequency data contaminated by microstructure noise is essential for obtaining consistent estimators of daily integrated beta, the analysis of these betas presents different aspects of asymptotic behavior compared to previous literature that uses at least monthly beta. To address these points, we establish asymptotic theorems for the proposed estimation procedure and further discuss how to conduct hypothesis tests.

The rest of the paper is organized as follows. In Section 2, we propose statistical inference procedures for the integrated beta. In Section 3, we suggest the DR Beta model and examine the parameter estimation procedure with their asymptotic theorems. In Section 4, we provide a simulation study to check the finite sample performance for the proposed estimators. In Section 5, we carry out an empirical study with the E-mini S&P 500 index futures and 50 individual stocks to investigate the advantage of the proposed model. In Section 6, we conclude. The proofs and supplementary materials are collected in the online Appendix.

2 Robust realized integrated beta estimator

2.1 Model setup

We first fix some notations that we will use. Let $\mathbb{R}_+ = [0, \infty)$ and $\mathbb{N}$ be the set of all positive integers. Let A_{ij} denote the (i, j)th element of a matrix A, $A^\top$ denote its transpose matrix, and $\det(A)$ denote the determinant of A. We use the superscripts c and d for the continuous and jump processes, respectively.

We consider the following diffusion regression model, as originally introduced in Mykland and Zhang (2006) (see also Li et al. (2017a); Li and Xiu (2016); Reiß et al. (2015)):

$$dX_{2,t} = \beta^c_{t-} dX^c_{1,t} + \beta^d_{t-} \Delta X^d_{1,t} + dV_t, \tag{2.1}$$

where X_2 is a dependent process, X_1 is a covariate process, and V is a residual process. Further, $X^c_{1,t}$ denotes the continuous part of the covariate process, and $\Delta X^d_{1,t}$ is its jump at time t. Then, β^c_t and β^d_t are the time-varying factor loadings with respect to the continuous and jump parts of X_1, respectively. We assume that $X_{1,t}$ and V_t admit the following Grigelionis decomposition of the forms:

$$\begin{aligned}
X_{1,t} &= X_{1,0} + \int_0^t \mu_{1,s} ds + \int_0^t \sigma_s dB_s + \mathfrak{d}_1 \mathbf{1}_{\{|\mathfrak{d}_1| \le 1\}} * (\mathfrak{p} - \mathfrak{q})_t + \mathfrak{d}_1 \mathbf{1}_{\{|\mathfrak{d}_1| > 1\}} * \mathfrak{p}_t, \\
V_t &= V_0 + \int_0^t \mu_{2,s} ds + \int_0^t q_s dW_s + \mathfrak{d}_2 \mathbf{1}_{\{|\mathfrak{d}_2| \le 1\}} * (\mathfrak{p} - \mathfrak{q})_t + \mathfrak{d}_2 \mathbf{1}_{\{|\mathfrak{d}_2| > 1\}} * \mathfrak{p}_t,
\end{aligned}$$

where $\mu_{1,t}$ and $\mu_{2,t}$ are càdlàg, progressively measurable, and locally bounded drifts, σ_t and q_t are adapted càdlàg processes, B_t and W_t are independent standard Brownian motions, $\mathfrak{p}$ is a Poisson random measure on $\mathbb{R}^+ \times E$, with the compensator $\mathfrak{q}(dt, dx) = dt \otimes \lambda(dx)$ and the Polish space $(E, \mathcal{E})$, λ is a σ-finite measure, $\mathfrak{d}_1$ and $\mathfrak{d}_2$ are predictable functions on $\Omega \times \mathbb{R}^+ \times E$. All random quantities above are defined on a fixed filtered probability space $(\Omega, \mathcal{F}, (\mathcal{F}_t)_{t \ge 0}, \mathbb{P})$. Furthermore, σ^2_t stays away from 0.

For the proposed time series regression model in (2.1), we assume that time-varying

market betas follow a stochastic process defined on $(\Omega, \mathcal{F}, P)$ as follows:

$$d\beta_t^c = \mu_{\beta,t}dt + \sigma_{\beta,t}dB_{\beta,t}, \tag{2.2}$$

where $\mu_{\beta,t}$ is progressively measurable and locally bounded drift, $\sigma_{\beta,t}$ is càdlàg, $B_{\beta,t}$ is a standard Brownian motion with $dB_{\beta,t}dW_t = 0$ and $dB_{\beta,t}dB_t = \rho_{\beta,t}dt$ a.s. To measure the daily market beta, we use the following integrated beta ($I\beta$):

$$I\beta_i = \int_{i-1}^{i} \beta_t^c dt, \quad i \in \mathbb{N}. \tag{2.3}$$

In this paper, the parameter of interest is the daily integrated beta. When the beta process is constant over time with no price jumps, the integrated beta returns to the usual market beta of the capital asset pricing model (CAPM). That is, the diffusion regression model includes the traditional discrete-time CAPM regression.

Remark 1. In this paper, we separate the continuous and jump parts and mainly consider the continuous part. We also investigate market betas corresponding to the jump part in the empirical study, which is calculated based on the jump beta estimation method suggested by Li et al. (2017b). However, unlike the beta for the continuous part, the beta for the jump part does not have significant time series structures (see Figure 7). Thus, we focus on the beta process for the continuous part.

For the high-frequency observations, one of the stylized features is that the transaction prices are polluted by the market microstructure noise due to the discreteness of the price, bid-ask spread bounce, and adverse selection effects, such as clearing costs (Aït-Sahalia and Yu, 2009). To reflect this, we assume that the observed log prices have the additive microstructure noise as follows:

$$Y_{1,i}^m = X_{1,t_i} + \epsilon_{1,i}^m \quad \text{and} \quad Y_{2,i}^m = X_{2,t_i} + \epsilon_{2,i}^m, \tag{2.4}$$

where $\epsilon_{1,i}^m$ and $\epsilon_{2,i}^m$ are the noise. Empirical studies reveal that the microstructure noise is dependent on the true price (Aït-Sahalia et al., 2011; Hansen and Lunde, 2006; Ubukata and

Oya, 2009) and has positive autocorrelation (Jacod et al., 2017; Li and Linton, 2022). To capture this, we allow microstructure noise to have a dependence on the true latent price, diurnal features, and polynomial decaying autocorrelation. Before describing our assumption about microstructure noise, we state the ρ-mixing property of a stationary random vector $\boldsymbol{\chi} = (\boldsymbol{\chi}_i)_{i\in\mathbb{Z}} = ((\chi_{1,i}, \chi_{2,i})^\top)_{i\in\mathbb{Z}}$.

Definition 1. *For a stationary process $\boldsymbol{\chi}$, let $\mathcal{G}_j = \sigma(\boldsymbol{\chi}_i : i \le j)$ and $\mathcal{G}^j = \sigma(\boldsymbol{\chi}_i : i \ge j)$ be the pre- and post-σ-fields at time j. A stationary process $\boldsymbol{\chi}$ is v-polynomially ρ-mixing if for some $C > 0$, $\rho_k(\boldsymbol{\chi}) \le C/k^v$ for all $k \ge 1$, where*

$$\begin{aligned}\rho_k(\boldsymbol{\chi}) \;=\; & \sup\big\{|\mathbb{E}(UV)| : U \text{ and } V \text{ are random variables, measurable with respect to} \\ & \mathcal{G}_0 \text{ and } \mathcal{G}^k, \text{ respectively}, \quad \mathbb{E}(U) = \mathbb{E}(V) = 0, \mathbb{E}(U^2) \le 1, \mathbb{E}(V^2) \le 1\big\}.\end{aligned}$$

Assumption 1. *The noise $(\boldsymbol{\epsilon}_i^m)_{i\in\mathbb{Z}} = ((\epsilon_{1,i}^m, \epsilon_{2,i}^m)^\top)_{i\in\mathbb{Z}}$ is realized as*

$$\epsilon_{1,i}^m = \vartheta_{1,t_i}\chi_{1,i} \quad \text{and} \quad \epsilon_{2,i}^m = \vartheta_{2,t_i}\chi_{2,i}, \tag{2.5}$$

where ϑ_1 and ϑ_2 are non-negative Itô semimartingales with locally bounded drift and càdlàg diffusion terms. Furthermore, $(\boldsymbol{\chi}_i)_{i\in\mathbb{Z}}$ is a stationary process, independent of the σ-field $\mathcal{F}_\infty = \bigvee_{t>0}\mathcal{F}_t$ and v-polynomially ρ-mixing for some $v \ge 5$. $\chi_{1,i}$ and $\chi_{2,i}$ are mean 0 and variance 1 with finite moments of all orders.

Remark 2. Assumption 1 implies that there exists a constant C such that $|r_{ab}(i)| \le \frac{C}{(|i|+1)^v}$ for all $i \in \mathbb{Z}$ and $a, b \in \{1, 2\}$, where $r_{ab}(i) = \mathbb{E}[\chi_{a,0}\chi_{b,i}]$. Thus, $R_{ab} = \sum_{i\in\mathbb{Z}} r_{ab}(i)$ is well defined.

2.2 Robust realized integrated beta estimator

When it comes to estimating the integrated beta based on the observed high-frequency financial data, there are a couple of obstacles. One is the microstructure noise, and the other is the intraday dynamics of the spot beta process. In this section, we discuss how to overcome these issues for the general stochastic beta process in (2.2).

For simplicity, we temporarily assume that the distance between adjacent observations is equal to $\Delta_m = 1/m$, where m is the number of high-frequency observations. We denote the high-frequency observed time points $t_l = l/m$ for $l = 1, \ldots, m$. This equally spaced observation time assumption can be easily extended to irregular observation time points. We discuss this later. To manage the intraday dynamics–that is, the time-varying spot beta process–we can use the following relationship:

$$\frac{d}{dt}[X^c_{2,t}, X^c_{1,t}] = \beta^c_t \frac{d}{dt}[X^c_{1,t}, X^c_{1,t}],$$

where $X^c_{2,t}$ is the continuous part of the individual asset log price process, and $[\cdot, \cdot]$ denotes the quadratic covariation. If β^c_t is identifiable–that is, the spot volatility of X^c_1 is nonzero–, we can obtain the spot beta by comparing the spot volatility of X^c_1 and the spot covolatility between X^c_1 and X^c_2 as follows:

$$\beta^c_t = \frac{\frac{d}{dt}[X^c_{2,t}, X^c_{1,t}]}{\frac{d}{dt}[X^c_{1,t}, X^c_{1,t}]}. \tag{2.6}$$

This is similar to the result of the usual regression coefficient, which is the covariance of the dependent and covariate variables over the variance of the covariate variable. The difference is that the spot beta is defined by the spot volatility and covolatility. Thus, it can represent the linear relationship at time t between the dependent and covariate processes. If the spot volatility and covolatility are constant over time, the spot beta is the same as the usual regression coefficient. By integrating the spot beta process, we finally obtain the integrated beta. Therefore, as long as the spot volatility estimators perform well, we can estimate the integrated beta.

To estimate spot volatilities, we employ the estimation method developed for estimating integrated volatility with microstructure noise (Aït-Sahalia et al., 2010; Barndorff-Nielsen et al., 2008, 2011; Christensen et al., 2010; Fan and Kim, 2018; Jacod et al., 2009, 2019; Shin et al., 2023; Xiu, 2010; Zhang, 2006; Zhang et al., 2005, 2016). In order to handle the autocorrelation structure of the microstructure noise, we employ the pre-averaging method in Jacod et al. (2019) as follows. We choose a sequence of integers, k_m, such that $k_m = C_k \Delta_m^{-1/2}$ for some positive constant C_k. We select a weight function $g(\cdot)$ on $[0, 1]$ satisfying that $g(\cdot)$

is continuous, piecewise continuously differentiable with a piecewise Lipschitz derivative g' with $g(0) = g(1) = 0$ and $\int_0^1 g^2(s)ds > 0$. Let

$$\phi_0(s) = \int_s^1 g(u)g(u-s)du,\ \psi_0 = \phi_0(0), \phi_1(s) = \int_s^1 g'(u)g'(u-s)du,\ \psi_1 = \phi_1(0),$$
$$\Phi_{00} = \int_0^1 \phi_0^2(s)ds,\ \Phi_{01} = \int_0^1 \phi_0(s)\phi_1(s)ds,\ \Phi_{11} = \int_0^1 \phi_1^2(s)ds.$$

We also choose a sequence of integers, l_m, such that $l_m = C_l \Delta_m^{-\varsigma}$ for some positive constant C_l and $\varsigma \in [\frac{1}{8}, \frac{1}{5}]$. Then, for $l = 1, \ldots, m$, $d = 1, \ldots, l_m$, and any processes P and P', we define

$$g_d^m = g\left(\frac{d}{k_m}\right), \quad P_l^m = P_{t_l}, \quad \widetilde{P}_l^m = \sum_{j=1}^{k_m-1} g_j^m \left(P_{l+j}^m - P_{l+j-1}^m\right), \quad \bar{P}_l^m = \frac{1}{l_m}\sum_{i=0}^{l_m-1} P_{l+i}^m,$$
$$\mathcal{E}_{PP',l}^{m,d} = \left(P_l^m - \bar{P}_{l+2l_m}^m\right)\left(P_{l+d}'^m - \bar{P}_{l+4l_m}'^m\right), \quad \mathcal{E}_{PP',l}^{m,-d} = \left(P_l'^m - \bar{P}_{l+2l_m}'^m\right)\left(P_{l+|d|}^m - \bar{P}_{l+4l_m}^m\right).$$

The spot covariance matrix $\mathbf{\Sigma}$ of $(X_1^c, X_2^c)^\top$ at time t_l is estimated with

$$\widehat{\mathbf{\Sigma}}_l^m = \widehat{\mathbf{\Sigma}}_{t_l} = \begin{pmatrix} v(Y_1, Y_1, u_{1,m}, u_{1,m}, t_l) & v(Y_1, Y_2, u_{1,m}, u_{2,m}, t_l) \\ v(Y_2, Y_1, u_{2,m}, u_{1,m}, t_l) & v(Y_2, Y_2, u_{2,m}, u_{2,m}, t_l) \end{pmatrix},$$

where

$$v(P, P', a, a', t_l) = \frac{1}{(b_m - 2k_m)\Delta_m k_m \psi_0}\left\{ \sum_{i=0}^{b_m-2k_m-1} \widetilde{P}_{l+i}^m \widetilde{P}_{l+i}'^m \mathbf{1}_{\{|\widetilde{P}_{l+i}^m| \le a,\, |\widetilde{P}_{l+i}'^m| \le a'\}} \right.$$
$$\left. - \frac{1}{k_m} \sum_{i=0}^{b_m-6l_m} \sum_{d=-k_m'}^{k_m'} \phi_d^m \mathcal{E}_{PP',l+i}^{m,d} \right\},$$
$$\phi_d^m = k_m \sum_{i \in \mathbb{Z}} \left(g_{i+1}^m - g_i^m\right)\left(g_{i-d+1}^m - g_{i-d}^m\right),$$

$b_m = C_b \Delta_m^{-\kappa}$, $k_m' = C_{k'} \Delta_m^{-\tau}$ for some positive constant C_b and $C_{k'}$, tuning parameters $\kappa \in (\frac{2}{3}, \frac{3}{4})$ and $\tau \in (\frac{1}{4v-4}, \frac{1}{8}]$, $u_{1,m}$ and $u_{2,m}$ are the thresholds chosen as $u_{1,m} = a_1(k_m\Delta_m)^{\varpi_1}$ and $u_{2,m} = a_2(k_m\Delta_m)^{\varpi_1}$ for some $a_1, a_2 > 0$, and $\varpi_1 \in (\frac{[v]-1}{2[v]-r}, \frac{2[v]-5}{4[v]-8})$ for r defined in Assumption 2(c). Under some mild conditions, we can show the consistency of the spot

volatility estimator (see Theorem 1 and Figueroa-López and Wu (2022)). Using the plug-in method, we can estimate the spot beta with the above spot volatility estimators. However, due to the microstructure noise, the functional form of the spot volatility estimators has a bias term. This fact prevents obtaining the asymptotic distribution with the convergence rate of $m^{-1/4}$ when estimating the integrated beta by the simple integration of the biased spot beta estimators. To overcome this, we introduce a bias adjustment scheme and construct a realized integrated beta (RIB) estimator as follows:

$$RIB_1 = \widehat{I\beta}_1 = b_m\Delta_m \sum_{i=0}^{\lfloor \frac{1}{b_m\Delta_m} \rfloor - 1} \left(\widehat{\beta}^m_{ib_m} - \widehat{B}^m_{ib_m} \right), \quad \widehat{\beta}^m_i = \frac{\widehat{\boldsymbol{\Sigma}}^m_{12,i}}{\widehat{\boldsymbol{\Sigma}}^{m,*}_{11,i}}, \quad \widehat{\boldsymbol{\Sigma}}^{m,*}_{11,i} = \max(\widehat{\boldsymbol{\Sigma}}^m_{11,i}, \delta_m), \tag{2.7}$$

where δ_m is a sequence of positive real numbers converging to zero and $\widehat{B}^m_{ib_m}$ is a de-biasing term of the form

$$\widehat{B}^m_i = \widehat{B}_{t_i} = \frac{4}{\psi_0^2 {C_k}^3 b_m \Delta_m^{1/2}} \left[\left(\frac{{C_k}^2 \Phi_{01}}{\widehat{\boldsymbol{\Sigma}}^{m,*}_{11,i}} + \frac{\Phi_{11} \widehat{\boldsymbol{\vartheta}}^m_{11,i}}{\left(\widehat{\boldsymbol{\Sigma}}^{m,*}_{11,i} \right)^2} \right) \left(\widehat{\boldsymbol{\vartheta}}^m_{11,i} \frac{\widehat{\boldsymbol{\Sigma}}^m_{12,i}}{\widehat{\boldsymbol{\Sigma}}^{m,*}_{11,i}} - \widehat{\boldsymbol{\vartheta}}^m_{12,i} \right) \right], \tag{2.8}$$

$$\widehat{\boldsymbol{\vartheta}}^m_{11,i} = (b_m - 6l_m)^{-1} \sum_{j=i}^{i+b_m-6l_m} \sum_{d=-k'_m}^{k'_m} \mathcal{E}^{m,d}_{Y_1Y_1,j}, \quad \widehat{\boldsymbol{\vartheta}}^m_{12,i} = (b_m - 6l_m)^{-1} \sum_{j=i}^{i+b_m-6l_m} \sum_{d=-k'_m}^{k'_m} \mathcal{E}^{m,d}_{Y_1Y_2,j},$$

$$\widehat{\boldsymbol{\vartheta}}^m_{22,i} = (b_m - 6l_m)^{-1} \sum_{j=i}^{i+b_m-6l_m} \sum_{d=-k'_m}^{k'_m} \mathcal{E}^{m,d}_{Y_2Y_2,j}.$$

We utilize $\widehat{\boldsymbol{\Sigma}}^{m,*}_{11,l}$ instead of $\widehat{\boldsymbol{\Sigma}}^m_{11,l}$ for estimating spot beta in order to prevent the denominator of $\widehat{\beta}^m_i$ from being a non-positive value. Thanks to the de-biasing term $\widehat{B}^m_{ib_m}$, the average form in (2.7) can achieve the optimal convergence rate $m^{-1/4}$.

Remark 3. The RIB estimator is developed along the lines of the estimators in Chen (2018); Jacod and Rosenbaum (2013), which proposed estimators of integrated volatility functionals. Specifically, Jacod and Rosenbaum (2013) considered the estimator in the absence of the microstructure noise, and Chen (2018) addressed the case of presence i.i.d. microstructure noise using the traditional pre-averaging scheme. The traditional pre-averaging scheme utilizes the property of diverging microstructure noise in the high-frequency returns to remove

the microstructure noise effect. However, in the presence of price-dependent and autocorrelated microstructure noise, this approach faces challenges. The RIB estimator, adapting the approach presented in Jacod et al. (2019), handles the dependent structure of microstructure noise by directly obtaining a proxy for the microstructure noise. Therefore, the RIB estimator is a consistent estimator of the integrated beta, whereas the others in Chen (2018); Jacod and Rosenbaum (2013) are not consistent estimators in the presence of price-dependent and autocorrelated microstructure noise. The consistency of estimators plays a crucial role in time series analysis, as it contributes to capturing the time series dynamics.

To investigate the asymptotic behavior of the RIB estimator, we need the following technical conditions.

Assumption 2.

(a) The processes σ_t and σ_t^{-1} are locally bounded.

(b) We have

$$\sigma_t^2 = \sigma_0^2 + \int_0^t \widetilde{\mu}_{1,s} ds + \int_0^t \widetilde{\sigma}_s d\widetilde{B}_s + \widetilde{\mathfrak{d}}_1 \mathbf{1}_{\{|\widetilde{\mathfrak{d}}_1| \leq 1\}} * (\mathfrak{p} - \mathfrak{q})_t + \widetilde{\mathfrak{d}}_1 \mathbf{1}_{\{|\widetilde{\mathfrak{d}}_1| > 1\}} * \mathfrak{p}_t \quad \textit{and}$$
$$q_t^2 = q_0^2 + \int_0^t \widetilde{\mu}_{2,s} ds + \int_0^t \widetilde{q}_s d\widetilde{W}_s + \widetilde{\mathfrak{d}}_2 \mathbf{1}_{\{|\widetilde{\mathfrak{d}}_2| \leq 1\}} * (\mathfrak{p} - \mathfrak{q})_t + \widetilde{\mathfrak{d}}_2 \mathbf{1}_{\{|\widetilde{\mathfrak{d}}_2| > 1\}} * \mathfrak{p}_t,$$

where $\widetilde{\mu}_{1,t}$ and $\widetilde{\mu}_{2,t}$ are progressively measurable and locally bounded drifts; $\widetilde{\sigma}_t$ and $\widetilde{q}_t$ are adapted càdlàg processes. The standard Brownian motions $\widetilde{B}_t$ and $\widetilde{W}_t$ satisfy almost surely

$$d\widetilde{B}_t dB_{\beta,t} = 0, \quad d\widetilde{B}_t dW_t = 0, \quad d\widetilde{B}_t d\widetilde{W}_t = 0, \quad d\widetilde{B}_t dB_t = \widetilde{\rho}_{1,t} dt,$$
$$d\widetilde{W}_t dB_{\beta,t} = 0, \quad d\widetilde{W}_t dB_t = 0, \quad d\widetilde{W}_t d\widetilde{B}_t = 0, \quad d\widetilde{W}_t dW_t = \widetilde{\rho}_{2,t} dt,$$

where $\widetilde{\rho}_{1,t}$ and $\widetilde{\rho}_{2,t}$ are bounded. The stochastic processes $\widetilde{\mu}_{1,t}, \widetilde{\mu}_{2,t}, \widetilde{\sigma}_t$, $\widetilde{q}_t$, $\widetilde{\rho}_{1,t}$, and $\widetilde{\rho}_{2,t}$ are defined on $(\Omega, \mathcal{F}, P)$.

(c) For some $r \in [0, \frac{2[v]-8}{2[v]-5})$, there are a sequence T_k of stopping times increasing to ∞, a sequence of deterministic nonnegative λ-integrable functions $\mathcal{J}_k$ on $\mathbb{R}^2$ such that

$|\mathfrak{d}_i(\omega,t,z)|^r \wedge 1 \leq \mathcal{J}_k(z)$, $\left|\beta^d_{t-}\mathfrak{d}_1(\omega,t,z)\right|^r \wedge 1 \leq \mathcal{J}_k(z)$ *and* $\left|\widetilde{\mathfrak{d}}_i(\omega,t,z)\right|^2 \wedge 1 \leq \mathcal{J}_k(z)$ *for* $i \in \{1,2\}$ *and all* (ω,t,z) *with* $t \leq T_k(\omega)$.

(d) If P_t *is one of the processes* $\widetilde{\sigma}_t$, $\widetilde{q}_t$, $\widetilde{\rho}_{1,t}$, *or* $\rho_{\beta,t}$, *then it satisfies the property (P-2), where*

(P-k) There exist $C > 0$, *such that* $\mathbb{E}\left[\sup_{u\in[t,t+s]}(P_u - P_t)^k|\mathcal{F}_t\right] \leq Cs$ *a.s. for any* $t, s \geq 0$.

Remark 4. The locally bounded condition of σ_t^{-1} in Assumption 2(a) is required to identify the beta from the processes. Assumption 2(c) is required to bound the degree of activity of jumps (Aït-Sahalia and Jacod, 2009). The parameter r should be less than $\frac{2[v]-8}{2[v]-5}$, whereas Jacod et al. (2019) requires $r < \frac{2[v]-4}{2[v]-3}$. This is because the RIB estimator requires the second-moment condition for the jump-truncation error, whereas Jacod et al. (2019) only requires convergence in probability for the jump-truncation error. If $\boldsymbol{\chi}$ is ρ-mixing with exponential decay rate, we only require $r < 1$. Assumption 2(d) holds for any Itô semimartingale process with bounded drift, diffusion, and jump terms.

The following theorem establishes the convergence rate and asymptotic distributions for the proposed RIB estimator.

Theorem 1. *Under Assumptions 1 and 2, we have*

$$m^{1/4}(RIB_1 - I\beta_1) \to \int_0^1 \mathcal{R}_s d\widetilde{Z}_s \quad \mathcal{F}_\infty\text{-stably as } m \to \infty,$$

where $\widetilde{Z}$ *is a standard Brownian motion independent of* $\mathcal{F}$, $\mathcal{R}_s$ *is the square root of*

$$\mathcal{R}_s = \frac{2}{\psi_0^2}\left(\Phi_{00}\frac{C_k q_s^2}{\sigma_s^2} + \Phi_{01}\frac{A_{1,s}}{C_k} + \Phi_{11}\frac{A_{2,s}}{{C_k}^3}\right),$$

and

$$\begin{aligned} A_{1,s} &= \frac{\vartheta_{1,s}^2 R_{11} q_s^2 - 2\beta_s^c \vartheta_{1,s}\vartheta_{2,s}R_{12} + \vartheta_{2,s}^2 R_{22}}{\sigma_s^2} + \vartheta_{1,s}^2 R_{11}(\beta_s^c)^2, \\ A_{2,s} &= \frac{\vartheta_{1,s}^2}{\sigma_s^4}\left(2(\beta_s^c)^2\vartheta_{1,s}^2 R_{11}^2 - 4\beta_s^c\vartheta_{1,s}\vartheta_{2,s}R_{11}R_{12} + \vartheta_2^2(R_{11}R_{22} + R_{12}^2)\right). \end{aligned}$$

Theorem 1 shows that the convergence rate of the RIB estimator is $m^{-1/4}$, which is known as the optimal rate with the presence of microstructure noise and establishes its asymptotic normality. To extend the estimator over all periods, we set m_i to be the total number of high-frequency observations for the ith day and rewrite $m = \sum_{i=1}^{n} m_i/n$. We further let the $t_{i,j}$'s be the high-frequency observed time points for the ith day, such that $i-1 = t_{i,0} < t_{i,1} < \cdots < t_{i,m_i} = i$, where $|t_{i,j} - t_{i,j-1}| = O\left(m^{-1}\right)$ for all i, j. Then, we can construct the RIB estimator as follows:

$$RIB_i = \frac{1}{m_i} \sum_{l=0}^{m_i - b_{m_i}} \left[\widehat{\beta}_{i,t_{i,l}} - \widehat{B}_{i,t_{i,l}} \right] \quad \text{and} \quad \widehat{\beta}_{i,t_{i,l}} = \frac{\widehat{\boldsymbol{\Sigma}}_{21,t_{i,l}}}{\max(\widehat{\boldsymbol{\Sigma}}_{22,t_{i,l}}, \delta_{m_i})}. \tag{2.9}$$

Moreover, we can show Theorem 1 for each RIB_i under the usual assumption in the asynchronous high-frequency data analysis (see Assumption 3(e)). We utilize these well-performing RIB estimators to analyze the dynamic structures of integrated betas in the following section.

To utilize the asymptotic distribution result, we need to construct a consistent asymptotic variance estimator. In the following proposition, we propose the asymptotic variance estimator and show its consistency.

Proposition 1. *Under Assumptions 1 and 2,* $\widehat{S}_m = b_m \Delta_m \sum_{i=0}^{\left[\frac{1}{b_m \Delta_m}\right]-1} \widehat{\mathcal{R}}^{2,m}_{ib_m}$ *is a consistent asymptotic variance estimator of the* RIB *estimator, where*

$$\begin{aligned}
\widehat{\mathcal{R}}^{2,m}_i \;=\; & \frac{2C_k}{\psi_0^2} \left[\Phi_{00} \left(\frac{\widehat{\boldsymbol{\Sigma}}^m_{22,i}}{\widehat{\boldsymbol{\Sigma}}^{m,*}_{11,i}} - \frac{(\widehat{\boldsymbol{\Sigma}}^m_{12,i})^2}{(\widehat{\boldsymbol{\Sigma}}^{m,*}_{11,i})^2} \right) + \frac{\Phi_{01}}{C_k^2} \left(\frac{\widehat{\boldsymbol{\vartheta}}^m_{22,i}}{\widehat{\boldsymbol{\Sigma}}^{m,*}_{11,i}} - \frac{2\widehat{\boldsymbol{\Sigma}}^m_{12,i}\widehat{\boldsymbol{\vartheta}}^m_{12,i}}{(\widehat{\boldsymbol{\Sigma}}^{m,*}_{11,i})^2} + \frac{\widehat{\boldsymbol{\Sigma}}^m_{22,i}\widehat{\boldsymbol{\vartheta}}^m_{11,i}}{(\widehat{\boldsymbol{\Sigma}}^{m,*}_{11,i})^2} \right) \\
& + \frac{\Phi_{11}}{C_k^3} \left(\frac{2(\widehat{\boldsymbol{\Sigma}}^m_{12,i}\widehat{\boldsymbol{\vartheta}}^m_{11,i})^2}{(\widehat{\boldsymbol{\Sigma}}^{m,*}_{11,i})^4} + \frac{\widehat{\boldsymbol{\vartheta}}^m_{11,i}\widehat{\boldsymbol{\vartheta}}^m_{12,i}}{(\widehat{\boldsymbol{\Sigma}}^{m,*}_{11,i})^2} - 4\frac{\widehat{\boldsymbol{\Sigma}}^m_{12,i}\widehat{\boldsymbol{\vartheta}}^m_{11,i}\widehat{\boldsymbol{\vartheta}}^m_{12,i}}{(\widehat{\boldsymbol{\Sigma}}^{m,*}_{11,i})^3} + \frac{(\widehat{\boldsymbol{\vartheta}}^m_{11,i})^2}{(\widehat{\boldsymbol{\Sigma}}^{m,*}_{11,i})^2} \right) \Bigg],
\end{aligned}$$

where $\widehat{\boldsymbol{\vartheta}}^m_{11,i}$, $\widehat{\boldsymbol{\vartheta}}^m_{12,i}$, *and* $\widehat{\boldsymbol{\vartheta}}^m_{12,i}$ *are defined in* (2.8). *That is, we have* $\widehat{S}_m \xrightarrow{p} \int_0^1 \mathcal{R}^2_s ds$.

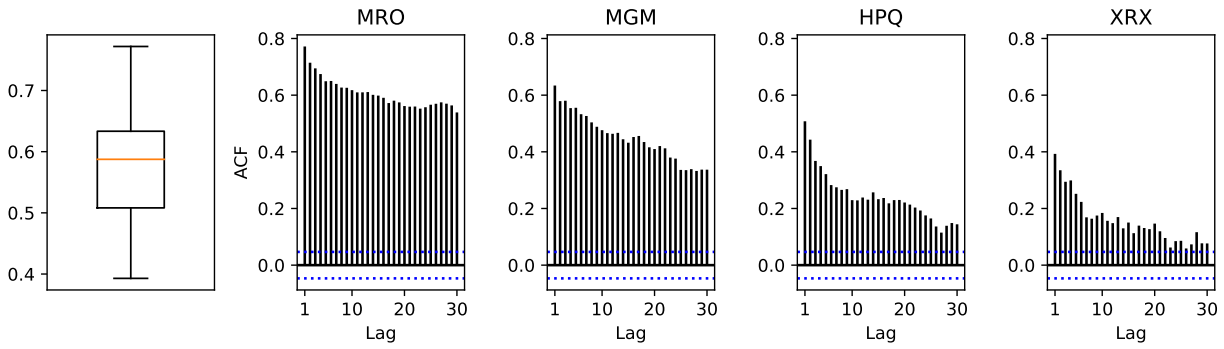

Figure 1: The box plot (left) of the first-order autocorrelations of the daily realized integrated betas for the top 50 large trading volume assets among the S&P 500 from January 1, 2010, to December 31, 2016, and the ACF plots for the largest, 75th, 25th, and smallest first-order autocorrelation among the 50 assets excluding outliers.

3 Dynamic analysis of integrated betas

3.1 Dynamic realized beta models

In this section, we conduct a dynamic analysis of integrated betas. To check the low-frequency time series structure of high-frequency-based market betas, we draw autocorrelation function (ACF) plots for daily realized integrated betas for the top 50 large trading volume stocks in Figure 1. Figure 1 shows that the realized beta has a persistent autoregressive structure. To account for this beta dynamics, we consider the ARMA(p, q) structure on integrated betas as follows:

$$I\beta_n = \omega + \sum_{i=1}^{p} \alpha_i I\beta_{n-i} + \sum_{i=1}^{q} \gamma_i D_{n-i} + D_n, \tag{3.1}$$

where $D_n = I\beta_n - h_n$ is martingale difference and h_n is $\mathcal{F}_{n-1}$-adapted. We call this dynamic realized beta (DR Beta) model. The model (3.1) is equivalent to the following model:

$$\begin{aligned} I\beta_n &= h_n(\theta) + D_n, \\ h_n(\theta) &= \omega + \sum_{i=1}^{q} \gamma_i^g h_{n-i}(\theta) + \sum_{i=1}^{p\vee q} \alpha_i^g I\beta_{n-i}, \end{aligned} \tag{3.2}$$

where $\gamma_i^g = -\gamma_i$, $\alpha_i^g = \alpha_i \mathbf{1}_{\{i \le p\}} + \gamma_i \mathbf{1}_{\{i \le q\}}$, and $\theta = (\omega, \gamma_1^g, \ldots, \gamma_q^g, \alpha_1^g, \ldots, \alpha_{p \vee q}^g)$ is model parameter. Since (3.2) is more practicable than (3.1), we focus on estimating parameters of (3.2).

3.2 Parametric estimation for the DR Beta model

3.2.1 Estimation procedure based on high-frequency data and a low-frequency structure

According to the strong autoregressive structure of the RIB_i's in Figure 1, we now assume that integrated market betas follow the DR Beta model defined in (3.2). To estimate the true parameters $\theta_0 = (\omega_0, \gamma_{0,1}^g, \ldots, \gamma_{0,q}^g, \alpha_{0,1}^g, \ldots, \alpha_{0,p \vee q}^g)$, we consider the well-known ordinary least squares (OLS) estimation, which compares the conditional expectations of integrated betas and its non-parametric estimators RIB_i's as follows:

$$L_{n,m}(\theta) = -\frac{1}{n} \sum_{i=1}^{n} \{RIB_i - h_i(\theta)\}^2 . \tag{3.3}$$

The difference between the $h_i(\theta)$ and the RIB_i can be decomposed into the martingale difference and the estimation error. The estimation error is asymptotically negligible. Furthermore, with some technical assumptions, the martingale difference terms have a negligible effect on the estimation result. Thus, the RIB estimator can be utilized as the proxy of $h_i(\theta)$. To harness the quasi-likelihood function above, we first need to evaluate the conditional expectation term $h_i(\theta)$. Unfortunately, the true integrated betas are not observable. Thus, we adopt their non-parametric estimators RIB_i to evaluate $h_i(\theta)$ as follows:

$$\widehat{h}_n(\theta) = \omega + \sum_{i=1}^{q} \gamma_i^g \widehat{h}_{n-i}(\theta) + \sum_{j=1}^{p \vee q} \alpha_j^g RIB_{n-j}.$$

Then, we define the quasi-likelihood function as follows:

$$\widehat{L}_{n,m}(\theta) = -\frac{1}{n} \sum_{i=1}^{n} \left\{ RIB_i - \widehat{h}_i(\theta) \right\}^2 , \tag{3.4}$$

and estimate the model parameters by maximizing the quasi-likelihood function $\widehat{L}_{n,m}(\theta)$ as follows:

$$\widehat{\theta} = \text{argmax}_{\theta\in\Theta}\, \widehat{L}_{n,m}(\theta),$$

where Θ is the parameter space of θ.

To estimate $\widehat{h}_i(\theta)$, we need initial values $\widehat{h}_0(\theta), \ldots, \widehat{h}_{-q+1}(\theta)$, and $RIB_0, \ldots, RIB_{-p\vee q+1}$, which we cannot obtain from given information whereas it is required to get $\widehat{h}_1(\theta), \ldots, \widehat{h}_{p\vee q}(\theta)$. Meanwhile, similar to Lemma 1 in Kim and Wang (2016), we can show that the dependence of $h_i(\theta)$ on initial values decays with the order n^{-1}. Thus, we can utilize, for example, $\frac{1}{n}\sum_{i=1}^{n} RIB_i$ as initial values.

3.2.2 Asymptotic theory

In this subsection, we establish asymptotic theorems for the proposed estimator $\widehat{\theta}$. We first define some notations. Define $\|A\|_{\max} = \max_{1\le i\le k, 1\le j\le k'} |A_{ij}|$ for a $k \times k'$ matrix A. Let $C > 0$ be generic constants whose values are free of n and m and may change from occurrence to occurrence.

To explore the asymptotic behaviors of $\widehat{\theta}$, the following technical conditions are required.

Assumption 3.

(a) Let

$$\begin{aligned}\Theta \;=\; & \{(\omega, \gamma_1^g, \ldots, \gamma_q^g, \alpha_1^g, \ldots, \alpha_{p\vee q}^g) : \omega_l < \omega < \omega_u,\ \gamma_l^g < \gamma_1^g, \ldots, \gamma_q^g < \gamma_u^g,\\ & \alpha_l^g < \alpha_1^g, \ldots, \alpha_{p\vee q}^g < \alpha_u^g, \sum_{i=1}^{q} |\gamma_i^g| < 1, \sum_{i=1}^{p\vee q} \left|\mathbf{1}_{\{i\le q\}}\gamma_i^g + \mathbf{1}_{\{i\le p\vee q\}}\alpha_i^g\right| < 1\},\end{aligned}$$

where $\omega_l, \omega_u, \alpha_l^g, \alpha_u^g, \gamma_l^g, \gamma_u^g$ are known constants such that $\alpha_l^g, \alpha_u^g, \gamma_l^g$ and γ_u^g are in $(-1, 1)$.

(b) For all $\theta \in \Theta$, $|\varphi_\theta(x)| = 0 \Rightarrow |x| > 1$, where $\varphi_\theta(x) = 1 - \sum_{i=1}^{p\vee q}(\mathbf{1}_{\{i\le q\}}\gamma_i^g + \mathbf{1}_{\{i\le p\vee q\}}\alpha_i^g)x^i$.

(c) $\Upsilon_{\theta_0}(x)$ does not have no common root with $\varphi_{\theta_0}(x)$, where $\Upsilon_\theta(x) = \sum_{i=1}^{1} \gamma_i^g x^i$.

(d) D_i is stationary ergodic process satisfying $\sup_{i\le n} \mathbb{E}\left[D_i^2 | \mathcal{F}_{i-1}\right] \le C$.

(e) There exist some fixed constants C_1, C_2 such that $C_1 m \leq m_i \leq C_2 m$, and $\sup_{1\leq j\leq m_i} |t_{i,j} - t_{i,j-1}| = O\left(m^{-1}\right)$ *and* $n^2 m^{-1} \to 0$ *as* $m, n \to \infty$.

(f) We have $\sup_{i\leq n} \mathbb{E}\left[|RIB_i - I\beta_i|^2\right] \leq C m^{-1/2}$.

Remark 5. Assumption 3(a)–(d) are usually imposed when analyzing asymptotic properties of the ARMA-type models. For example, Assumption 3(b) implies the stationarity of $I\beta_i$ and $h_i(\theta)$, and Assumption 3(c) is required to identify the parameter space. Finally, Assumption 3(f) is required to handle the estimation errors of the unobserved integrated betas. Under some bounded moment conditions on the random quantities, we can show that Assumption 3(f) holds. We elaborate on conditions of the long-span asymptotic behavior of the RIB estimator in Assumption 4.

The following theorems provide the asymptotic results including the convergence rate and asymptotic normality for the proposed parameters $\widehat{\theta}$.

Theorem 2. *Under Assumption 3 (except for $n^2 m^{-1} \to 0$), we have*

$$\|\widehat{\theta} - \theta_0\|_{max} = O_p(m^{-1/4} + n^{-1/2}).$$

Theorem 3. *Under Assumption 3, we have, as $m, n \to \infty$,*

$$\sqrt{n}(\widehat{\theta} - \theta_0) \xrightarrow{d} N(0, V),$$

where

$$V = \mathbb{E}\left[D_1^2\right] \left(\mathbb{E}\left[\frac{\partial h_1(\theta)}{\partial \theta} \frac{\partial h_1(\theta)}{\partial \theta^\top}\bigg|_{\theta=\theta_0} \right] \right)^{-1}. \tag{3.5}$$

Remark 6. Theorem 2 shows that the quasi-maximum likelihood estimator $\widehat{\theta}$ has the converge rate $m^{-1/4} + n^{-1/2}$. The first term $m^{-1/4}$ comes from estimating the integrated beta, which is known as the optimal convergence rate with the presence of market microstructure noise. The second term $n^{-1/2}$ is the typical parametric convergence rate based on the low-frequency observations. Theorem 3 establishes the asymptotic normality of $\widehat{\theta}$.

In the asymptotic analysis of low-frequency dynamics, the sample size, n, is allowed to go to infinity. Thus, we need the long-span asymptotic behavior of the RIB estimator, such as Assumption 3(f). However, this condition is not satisfied under the locally bounded condition such as Assumption 2. To coincide with the asymptotic results of the proposed estimation procedures, we investigate the long-span asymptotic behavior of RIB as follows.

Assumption 4.

(a) We have bounded 64th moment of $\sigma, \mu_1, \mathfrak{d}_1, \beta^c, \beta^d, \mu_\beta$, *and* σ_β *and bounded 32nd moment of* $\sigma^{-1}, \widetilde{\mu}_1, \widetilde{\sigma}, \widetilde{\mathfrak{d}}_1, \vartheta_1, \vartheta_2, \mu_2, q$, *and* $\mathfrak{d}_2$.

(b) The process μ_1 *satisfies (P-64) and the processes* μ_2, ϑ_1, *and* ϑ_2 *satisfy (P-32) in Assumption 2(d).*

(c) For some $r \in [0, \frac{2[v]-8}{2[v]-5})$, *there are deterministic nonnegative* λ*-integrable functions* $\mathcal{J}$ *on* $\mathbb{R}^2$ *such that*

$$\begin{aligned}
&\mathbb{E}[|\mathfrak{d}_1(t,z)|^r \wedge 1] \vee \mathbb{E}[|\mathfrak{d}_2(t,z)|^r \wedge 1] \vee \mathbb{E}[|\beta^d_{t-}\mathfrak{d}_1(t,z)|^r \wedge 1] \leq \mathcal{J}(z),\\
&\mathbb{E}[|\widetilde{\mathfrak{d}}_1(t,z)|^2 \wedge 1] \vee \mathbb{E}[|\widetilde{\mathfrak{d}}_2(t,z)|^2 \wedge 1] \leq \mathcal{J}(z),\\
&\mathbb{E}[|\mathfrak{d}_1(t,z)|^{64}] \vee \mathbb{E}[|\mathfrak{d}_2(t,z)|^{32}] \vee \mathbb{E}[|\widetilde{\mathfrak{d}}_2(t,z)|^{32}] \vee \mathbb{E}[|\widetilde{\mathfrak{d}}_1(t,z)|^{32}] \leq \mathcal{J}(z).
\end{aligned}$$

Remark 7. To establish the convergence in the second mean in Theorem 4, we need moment conditions on the spot error terms. For example, we consider the squared error of the debiasing term, $(\widehat{B}^m_{ib_m} - B^m_{ib_m})^2$, from which the highest order error terms comes, where $B^m_{ib_m}$ is defined in the online Appendix equation (F.1). Technically, after applying Talyor's theorem, $(\widehat{B}^m_{ib_m} - B^m_{ib_m})^2$ become an octic function of the errors of spot variations with denominator, since $\widehat{B}^m_{ib_m}$ is a cubic function of estimated spot variations with denominator. Thus, we need 16th-moment conditions (32nd-moment conditions) on spot variation terms (drift and diffusion terms). Further, β^c and β^d are random processes which are multiplied by dX^c_1 and dX^d_1. Therefore, we need 64th moment conditions for some random quantities. If we assume that σ_t^{-1} is bounded, then we can reduce the 64th and 32nd-moment conditions in Assumptions 4(a), (b), and (c) by half, since we need one less Hölder's inequality. On the

other hand, unlike the case of asset price processes, it is economically sensible to consider the random quantities in Assumption 4 as mean-reverting processes. When a mean-reverting process follows a generalized Ornstein-Uhlenbeck process with Brownian motion, the high-order moment condition, such as Assumption 4, can be satisfied. Thus, it is not restrictive.

The following theorem establishes the long-span asymptotic behavior for the proposed RIB estimator.

Theorem 4. *Under Assumptions 1, 2(b) and (d), and 4 with $v \geq 7$, we have for $\delta_m = C_\delta \Delta_m^{\frac{1-\kappa}{16}}$ defined in* (2.7),

$$\sup_{i \in \mathbb{N}} \mathbb{E}\left[(RIB_i - I\beta_i)^2\right] \leq Cm^{-1/2}.$$

Theorem 4 shows that under some moment conditions, Assumption 3(f) is satisfied. That is, the condition in Assumption 3(f) can be replaced by Assumption 4.

3.2.3 Hypothesis tests

In financial practices, we are interested in model validity and making statistical inferences, such as hypothesis tests. To do this, we can harness the asymptotic normality result in Theorem 3 as follows:

$$T_n = \sqrt{n}\widehat{V}^{-1/2}(\widehat{\theta} - \theta_0) \xrightarrow{d} N(0, \mathbf{I}),$$

where $\widehat{V}$ is a consistent estimator of the asymptotic variance V defined in (3.5), and $\mathbf{I}$ is a $A \times A$ identical matrix, where $A = p \vee q + q + 1$. Then, with the test statistics T_n, we can conduct hypothesis tests based on the standard normal distribution. To evaluate the statistics T_n, we use the following asymptotic variance estimator,

$$\widehat{V} = \frac{1}{n}\sum_{i=1}^{n}\left\{RIB_i - \widehat{h}_i(\widehat{\theta})\right\}^2 \left(\frac{1}{n}\sum_{j=1}^{n}\frac{\partial \widehat{h}_j(\widehat{\theta})}{\partial \theta}\frac{\partial \widehat{h}_j(\widehat{\theta})^\top}{\partial \theta}\right)^{-1}. \tag{3.6}$$

Its consistency can be derived similarly to the proof of Theorem 3.

4 A simulation study

We conducted simulations to check the finite sample performance of the proposed statistical inference procedures. For simplicity, we chose $p = q = 1$ for the DR Beta model. In the online Appendix, we provide a high-frequency data-generating process of the beta diffusion process, whose integrated beta follows the DR Beta model. Using this data-generating process, we generated the beta processes $\beta^c_{t_{i,j}}$ and the jump-diffusion processes $X_{1,t_{i,j}}$ and $X_{2,t_{i,j}}$ for $t_{i,j} = i - 1 + j/m$, $i = 1, 2, \ldots, n$, $j = 1, 2, \ldots, m$ as follows:

$$
\begin{aligned}
&dX_{2,t} = \beta^c_t(\theta) dX^c_{1,t} + \beta^d_t J_{1,t} d\Lambda_{1,t} + dV_t, \\
&dX_{1,t} = \sigma_t dB_t + J_{1,t} d\Lambda_{1,t}, \quad dV_t = q_t dW_t + J_{2,t} d\Lambda_{2,t}, \\
&d\beta^c_t(\theta) = \left\{ 2\left(t - [t]\right)\left(\omega_1 + \gamma_1 \beta^c_{[t]}(\theta)\right) - \left(\omega_2 + \beta^c_{[t]}(\theta)\right) - \nu(Z_t - Z_{[t]}) + \alpha_1 \beta^c_t(\theta) \right\} dt \\
&\qquad\qquad + \nu\left([t] + 1 - t\right) dZ_t, \\
&dZ_t dB_t = dZ_t dW_t = dB_t dW_t = 0,
\end{aligned}
\tag{4.1}
$$

where $(\omega_1, \omega_2, \gamma_1, \alpha_1, \nu) = (-1.0, -1.5, 0.6, 0.2, 0.9)$, $q_t = 0.008$, and B_t, Z_t, and W_t are standard Brownian motions. The parameters ω_1 and ω_2 control the deterministic quadratic time-trend of the spot beta process, thereby determining its mean level. The persistent feature of the beta process is governed by the parameters γ_1 and α_1, with α_1 playing a key role in regulating the intraday level autoregressive characteristic of the spot beta process. The parameter ν controls the degree of intraday variation in the beta process. More detailed explanations of the process and its properties can be found in the online Appendix. With the chosen diffusion process parameters, the parameter of the DR Beta model becomes $\theta_0 = (\omega^g_0, \gamma_0, \alpha^g_0) = (0.84, 0.20,\ 0.50)$. We generated the individual asset log price process $X_{1,t}$ based on the realized GARCH-Itô model (Song et al., 2021) as follows:

$$
\begin{aligned}
d\sigma^2_t \;=\; & \left\{ 2\widetilde{\gamma}(t - \lceil t-1 \rceil)(\widetilde{\omega}_1 + \sigma^2_{\lceil t-1 \rceil}) - (\widetilde{\omega}_2 + \sigma^2_{\lceil t-1 \rceil}) + \widetilde{\alpha}\sigma^2_t - \widetilde{\nu}\widetilde{Z}^2_t \right\} dt \\
& + \widetilde{\beta} J^2_{1,t} d\Lambda_{1,t} + 2\widetilde{\nu}(\lceil t-1 \rceil + 1 - t)\widetilde{Z}_t d\widetilde{B}_t,
\end{aligned}
$$

where a standard Brownian motion $\widetilde{B}_t$ satisfies $d\widetilde{B}_t dW_t = d\widetilde{B}_t dU_t = 0, d\widetilde{B}_t dB_t = \widetilde{\rho} dt$, $(\widetilde{\omega}_1, \widetilde{\omega}_2, \widetilde{\gamma}, \widetilde{\alpha}, \widetilde{\beta}, \widetilde{\nu}, \widetilde{\rho}) = (6.04 \times 10^{-5}, 9.00 \times 10^{-6}, 0.35, 0.4, 0.1, 1 \times 10^{-5}, -0.5)$, and $\widetilde{Z}_t = \widetilde{B}_t - \widetilde{B}_{\lceil t-1 \rceil}$. The initial values for the simulation data were chosen to be $\beta_0^c(\theta) = \mathbb{E}\left[\beta_1^c(\theta)\right] = 2.72$, $\sigma_0^2 = \mathbb{E}\left[\sigma_1^2\right] = 7.55 \times 10^{-5}$, $X_{1,0} = 16$, and $X_{2,0} = 10$. For the jump part, we consider the finite activity jumps. Specifically, $\Lambda_{1,t}$ is a standard Poisson process with the intensities $\lambda_{1,t} = 5$ and $\lambda_{2,t} = 1$, and the jump sizes $J_{1,t}$ and $J_{2,t}$ were generated as follows:

$$J_{1,t}^2 = \max(4 \times 10^{-5} + M_{1,t}, \quad 4 \times 10^{-6}) \quad \text{and} \quad J_{2,t}^2 = \max(8 \times 10^{-6} + M_{2,t}, \quad 8 \times 10^{-7}),$$

where $M_{1,t}$ and $M_{2,t}$ follow $N(0, (5.5 \times 10^{-6})^2)$ and $N(0, (1 \times 10^{-6})^2)$, respectively. For each $J_{1,t}$ and $J_{2,t}$, we further assigned a positive (negative) sign with probability 0.5 to make a positive (negative) jump. Finally, β_t^d was chosen to be 2.4, and we generated Brownian motions using the Euler scheme.

The noisy high-frequency data $Y_{1,t_{i,j}}$ and $Y_{2,t_{i,j}}$ were generated from the model (2.4), where the true log price processes $X_{1,t_{i,j}}$ and $X_{2,t_{i,j}}$ were generated from (4.1), and the microstructure noise $\epsilon_{1,t_{i,j}}$ and $\epsilon_{2,t_{i,j}}$ follow (2.5), where $\vartheta_{1,t}$, $\vartheta_{2,t}$, and $\boldsymbol{\chi}_i$ follow Ornstein–Uhlenbeck-type processes with an U-shaped pattern and the AR(1) process with Gaussian innovations as follows:

$$\begin{aligned}
&d\vartheta_{1,t} = 10(\mu_{\vartheta_1,t} - \vartheta_{1,t})dt + s_1 dB_t, \quad d\vartheta_{2,t} = 10(\mu_{\vartheta_2,t} - \vartheta_{2,t})dt + 0.6 s_2 dB_t + 0.8 s_2 dW_t, \\
&\mu_{\vartheta_1,t} = s_1(1 + 0.1\cos(2\pi t)), \quad \mu_{\vartheta_2,t} = s_2(1 + 0.1\cos(2\pi t)), \\
&s_1 = 2.234 \times 10^{-4}, \quad s_2 = 5.464 \times 10^{-3}, \\
&\boldsymbol{\chi}_i = \begin{pmatrix} 0.5 & 0.1 \\ 0.1 & 0.5 \end{pmatrix} \boldsymbol{\chi}_{i-1} + e_i, \quad e_i \sim_{i.i.d.} N\left[\begin{pmatrix} 0 \\ 0 \end{pmatrix}, \begin{pmatrix} 0.815 & -0.652 \\ -0.652 & 0.815 \end{pmatrix} \right].
\end{aligned}$$

In this specification of the noise, the noise-to-signal ratio in the returns is predominantly determined by the parameters s_1 and s_2. Additionally, the cross-autocovariance structure of the noise is influenced by the VAR coefficients and the covariance of their innovations. This simulation setting satisfies Assumptions 3(a)–(f), and specifically, Assumption 3(f) can be verified by confirming that it aligns with Assumption 4. We repeated the simulation

process 1000 times. We normalized one second to 1/23400 so that the unit time contains 6.5 hours. For each simulation process, we generated high-frequency data with $m = 23400$ for 500 consecutive days and used the subsampled log prices of the last $n = 125, 250, 500$ days with high-frequency observations $m = 7800, 11700, 23400$ per day.

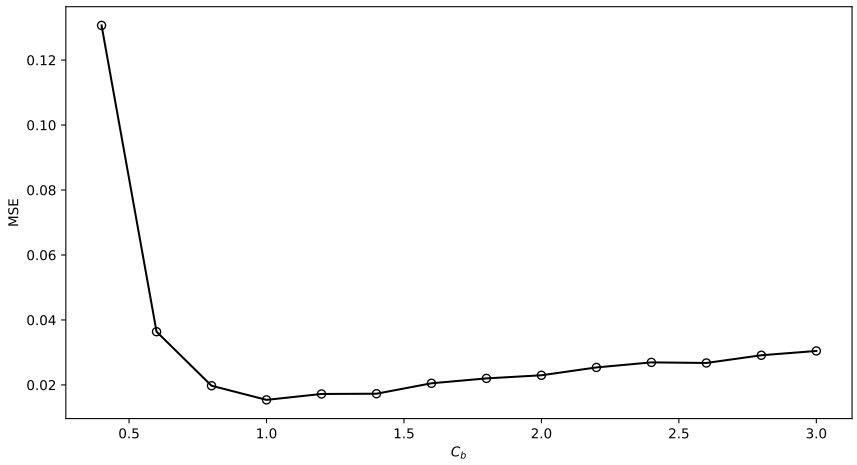

Figure 2: The MSEs of RIB estimator with $m = 23400$ against varying C_b.

For the RIB estimator, we used the usual triangular weight function $g(x) = \{x \wedge (1-x)\}$, and set $k_m = [\Delta_m^{-0.5}]$ and $\varpi_1 = 0.47$ as recommended by Christensen et al. (2010) and Aït-Sahalia and Xiu (2016), respectively. For each estimation of the daily integrated beta, we chose l_m using the heuristic criterion presented in Section 5.1.2 of Jacod et al. (2017), where the distance between two sequences is measured as the sum of their squared differences. To determine k'_m, we utilized the test for autocovariance of noise as presented in Corollary 3.5 in Jacod et al. (2017). Details can be found in the online Appendix A. In addition, for the truncation, we chose a_1 and a_2 as four times the sample standard deviation of the pre-averaged prices $k_m^{-1/2}\widetilde{Y}^m_{1,t_{d,k}}$ and $k_m^{-1/2}\widetilde{Y}^m_{2,t_{d,k}}$, respectively. We then needed to determine C_b. To do this, we checked the effect of the choice of C_b of the RIB estimator. Figure 2 depicts the estimated mean squared errors (MSE) of the RIB estimator with $m = 23400$ against varying C_b from 0.4 to 3.0, where $\kappa = 0.67$ and the integrated beta $I\beta_i$ is calculated as the Riemann sum of the true beta values for each trading days. From Figure 2, we find that for $C_b < 1$, the MSEs decrease as C_b increases, and for $C_b \geq 1$, the MSEs slightly

increase as C_b increases. This may be because the window size for the spot betas should be large enough to estimate spot betas, but too large a window size hinders the capture of the intraday dynamics of the beta processes. From this analysis, we set $C_b = 1$.

We first checked the performance of the non-parametric integrated beta estimator, RIB, proposed in Section 2.2. For comparison, we employed other integrated beta estimators proposed by Chen (2018) and Christensen et al. (2010). Chen (2018) proposed the estimator for volatility functionals and the integrated beta (CHEN) is a specific example. Christensen et al. (2010) calculated the integrated beta as a ratio of the integrated covariance between assets and systematic factors to the integrated variation of systematic factors. The proposed estimator utilizes a pre-averaged realized covariance estimator that is robust to i.i.d. microstructure noise but is not to autocorrelated noise and price jump. On the other hand, Jacod et al. (2019) proposed a robust pre-averaged integrated volatility estimator that is robust to price-dependent and autocorrelated microstructure noise and price jump. We employed the integrated beta estimator (PRVB), which adopts the robust pre-averaging integrated volatility estimator of Jacod et al. (2019) as the input of the integrated beta estimator in Christensen et al. (2010). The details of estimators can be found in the online Appendix C. We note that PRVB is a consistent estimator of the ratio of the integrated covariance between assets and systematic factors to the integrated variation of systematic factors. That is, while PRVB is a consistent estimator of the integrated beta when the intraday beta or market volatility is constant over time, the PRVB is not a consistent estimator of the integrated beta in general. On the other hand, CHEN is designed for estimating time-varying beta, but it does not consider the autocorrelated microstructure noise. Figure 3 shows the MSEs of the non-parametric integrated beta estimators, RIB, CHEN, and PRVB, for $m = 7800, 11700, 23400$. We note that the average value of the true integrated beta was 2.802. Figure 3 shows that the MSEs of RIB and PRVB decrease as the number of high-frequency observations increases, whereas the MSEs of CHEN do not. This is because the RIB and PRVB estimators can account for the autocorrelation structure of the microstructure noise, whereas CHEN fails to handle it. Further, RIB and CHEN perform better than PRVB since PRVB fails to deal with the time-varying beta. The magnitude of

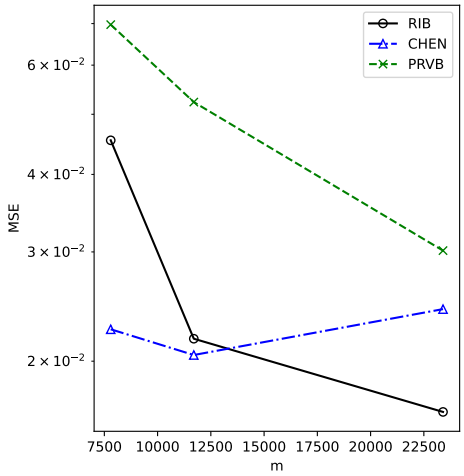

Figure 3: The MSEs of RIB, CHEN, and PRVB for $m = 7800, 11700, 23400$. The average value of the true integrated beta was 2.802.

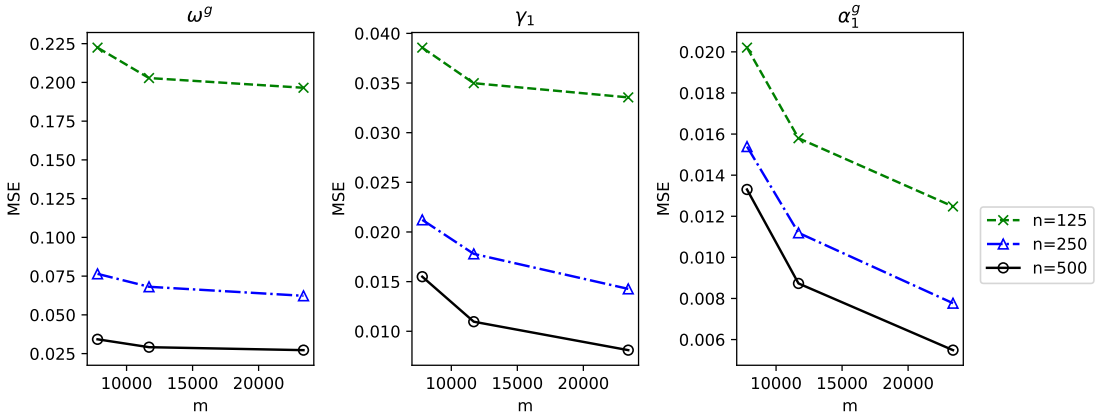

Figure 4: The MSEs of the least squared estimates with $m = 2340, 4680, 23400$ and $n = 100, 250, 500$.

the difference in performance between the RIB and PRVB estimators may depend on how volatile the intraday beta and market volatility processes are. When comparing the performances of the RIB and CHEN, the RIB estimator shows better performance for $m = 23400$, while CHEN does for $m = 7800, 11700$. It may be because the effect of the autocorrelated microstructure noise increases as m increases, while the estimation variance of the denoise term of RIB, which decreases as m increases, is larger than that of CHEN. These results support the theoretical results derived in Section 2.2.

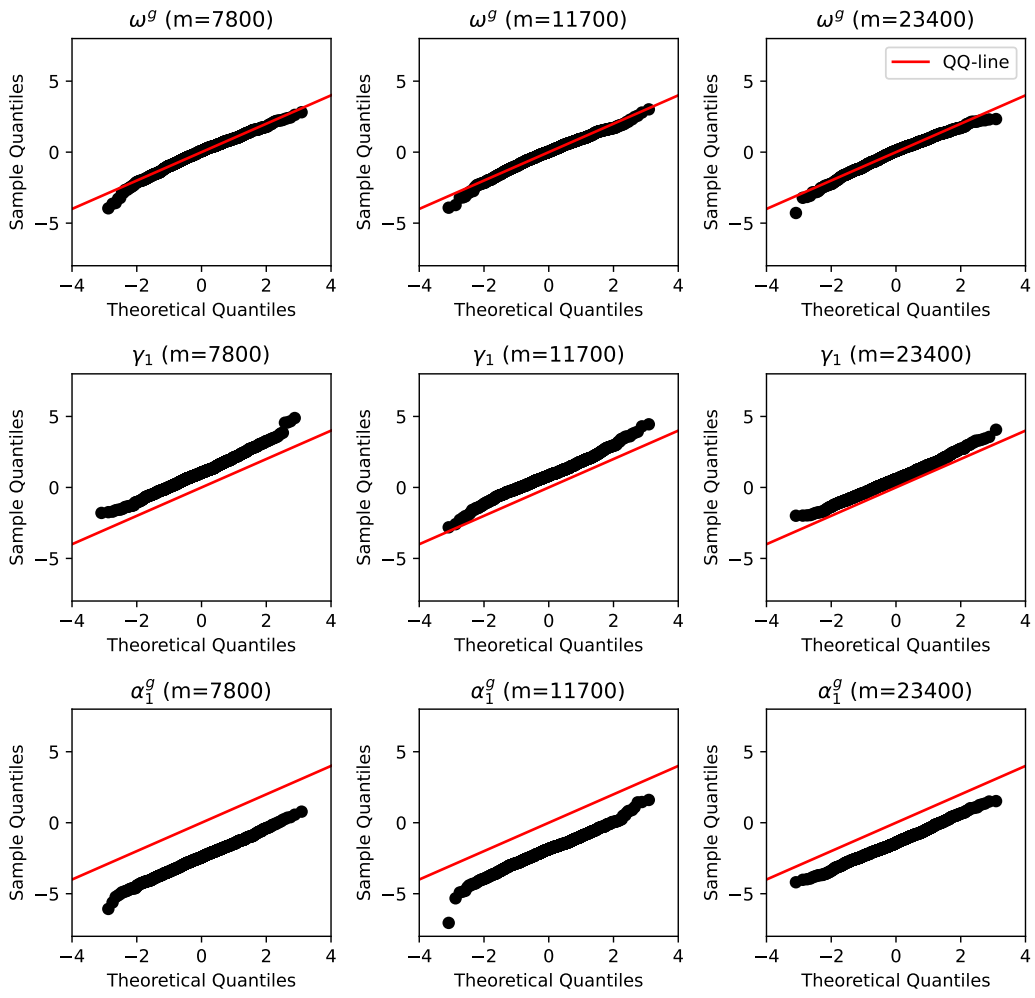

Figure 5: The standard normal (original) quantile-quantile plots of the Z-statistics estimates of ω^g, γ_1, and α_1^g for $n = 500$, $m = 7800, 11700, 23400$.

Next, we checked the finite sample performances of the proposed DR Beta model. We first estimated the model parameters using the proposed quasi-maximum likelihood estimation in Section 3.2 for $n = 100$, 250, 500 and $m = 7800, 11700, 23400$. To estimate $\widehat{h}_i(\theta)$, we set initial values $\widehat{h}_0(\theta) = RIB_0 = \frac{1}{n}\sum_{i=1}^{n} RIB_i$. Figure 4 draws the MSEs of the least squared estimates $\widehat{\theta}$'s for the model parameter θ_0. From Figure 4, we find that the MSEs decrease as n or m increases. These results match the theoretical findings in Section 3.2.

To check the asymptotic normality of the model parameters $(\omega^g, \gamma_1, \alpha_1^g)$, we calculated the Z-statistics proposed in Section 3.2.3. Figure 5 shows standard normal quantile-quantile

plots of the Z-statistics estimates of ω_1^g, γ_1, and α_1^g for $n = 500$ and $m = 7800, 11700, 23400$. From Figure 5, we find that the Z-statistics close to the standard normal distribution as m increases–that is, the non-parametric integrated beta estimator RIB closes to the true integrated beta $I\beta$. This result agrees with the theoretical findings in Section 3. Thus, based on the proposed Z-statistics, we can conduct hypothesis tests for the model parameters using the standard normal distribution.

The DR Beta model is an ARMA model for the integrated beta, utilizing the RIB, which is a consistent estimator of the integrated beta. One of the advantages of employing this consistent estimator to predict future market betas lies in its ability to effectively capture the low-frequency autoregressive dynamic structure, which helps improve the predictability of future beta values. Thus, we examined the out-of-sample performance of estimating the one-day-ahead conditional expected integrated beta $h_{n+1}(\theta_0)$ to check the predictability of the DR Beta model. We compared the DR Beta with three parametric models that employ high-frequency data and two parametric models that use low-frequency data. For the parametric model with high-frequency data, we considered the ARMA$(1, 1)$ models, which utilize CHEN (ARMAC) or PRVB (ARMAP) as daily realized beta, and Realized Beta GARCH (RBG) model (Hansen et al., 2014), which is a multivariate GARCH model utilizing realized measures of volatility and correlation. For the input covariance matrix of the RBG model, we used realized covariance, the sum of squared log-returns, with 5-min, 1-min, and 30-sec data ($m = 78, 390, 780$, respectively) to reduce the impact of the microstructure noise. We also used the robust pre-averaging realized covariance (Jacod et al., 2019) as the input of the RBG model (PRBG). Details of the RBG model can be found in Hansen et al. (2014). For the parametric models with low-frequency data, we used the dynamic conditional beta (DCB) model framework proposed by Engle (2016). Specifically, the beta prediction can be established by comparing the conditional covariance between assets and systematic factors to the conditional variance of systematic factors. The details of the procedure can be found in the online Appendix C. We employed the BEKK(1,1) and DCC(1,1) models as the conditional covariance matrix models, as suggested by Engle and Kroner (1995) and Bali and Engle (2010), respectively. We call the beta estimators with BEKK(1,1) and DCC(1,1)

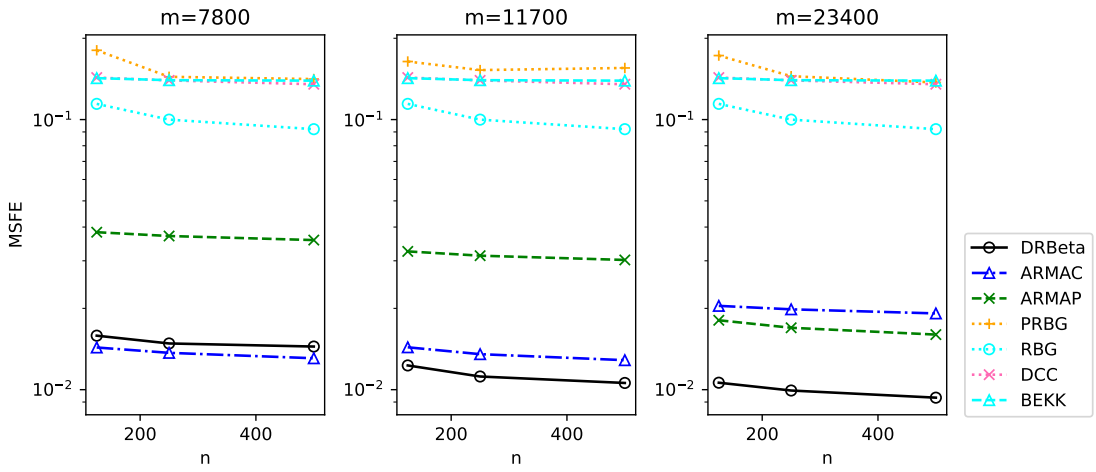

Figure 6: The MSFEs of DR Beta, ARMAC, ARMAP, PRBG, RBG, DCC, and BEKK with $n = 100, 250, 500$ and $m = 7800, 11700, 23400$. The average value of $h_{501,i}(\theta_0)$ was 2.813.

BEKK and DCC, respectively. For each model, we calculated the mean squared forecast errors (MSFEs) with the one-day-ahead forecasted beta across 1000 repeated simulations as follows:

$$\frac{1}{1000}\sum_{i=1}^{1000}\left(\widehat{Beta}_{n+1,i} - h_{n+1,i}(\theta_0)\right)^2,$$

where $h_{n+1,i}(\theta_0)$ is the true conditional expectation of the $(n+1)$th integrated beta and $\widehat{Beta}_{n+1,i}$ denotes one of the forecasted beta obtained using a parametric model such as DR Beta, ARMAC, ARMAP, PRBG, RBG, DCC, and BEKK models at the ith sample-path given the available information at time n. We note that the target of the benchmarks, except for ARMAC, is the ratio of the integrated covariance between assets and systematic factors to the integrated variation of systematic factors. Therefore, the MSFEs of the benchmarks additionally include the error from the discrepancy between the true integrated beta and the true ratio of the integrated covariance between assets and systematic factors to the integrated variation of systematic factors. In Figure 6, the MSFEs of DR Beta, ARMAC, ARMAP, PRBG, RBG, DCC, and BEKK are plotted for $n = 100, 250, 500$ and $m = 7800, 11700, 23400$. The average value of the true conditional expectation of 501st integrated beta was 2.813. For the RBG model, we plotted only the MSFEs with $m = 780$, which is the lowest MSFEs among $m = 78, 390, 780$. Figure 6 shows the MSFEs of the DR Beta

and ARMAP decrease as n or m increases, but other estimators do not have any strong pattern. This may be because the other benchmarks cannot account for the autocorrelated microstructure noise well. When comparing the DR Beta and ARMAP models, the DR Beta consistently outperforms the ARMAP. This is because the target variable of the PRVB estimator differs from the integrated beta under the time-varying spot beta and market volatility processes, thereby resulting in a less effective capture of integrated beta dynamics by the ARMAP model. Meanwhile, the high-frequency-based ARMA models show better performance than other competitors. When comparing the high-frequency-based ARMA models, the ARMAC and the DR Beta models show the best performance for $m = 7800$ and $m = 11700, 23400$, respectively, even though the CHEN has lower MSEs than the RIB for $m = 11700$. This may be because CHEN cannot account for the autocorrelation structure of the microstructure noise, which may cause some bias in the integrated beta estimation. From this result, we can conclude that estimating the ratio of integrated covariance to integrated variance cannot be a good proxy of integrated beta and the robust non-parametric integrated beta estimator helps account for the market beta dynamics.

We end this section by remarking that the proposed RIB estimator is not only a consistent estimator of the integrated beta under autocorrelated microstructure noise but also consistent even in the absence of autocorrelation in microstructure noise. To assess the finite sample performance of the proposed estimator when the microstructure noise has zero autocorrelation structure, we conducted an additional analysis under a setting of zero autocorrelation in the microstructure noise and fixed all other parameters. The full methodology and results of this analysis are presented in the online Appendix D.

5 Empirical analysis

In this section, we apply the proposed DR Beta model to real high-frequency trading data. We obtained high-frequency data for the top 50 large trading volume stocks among the S&P 500 from the TAQ database in the Wharton Research Data Services (WRDS) system from January 1, 2010, to December 31, 2016, 1762 trading days in total. We used the E-mini S&P

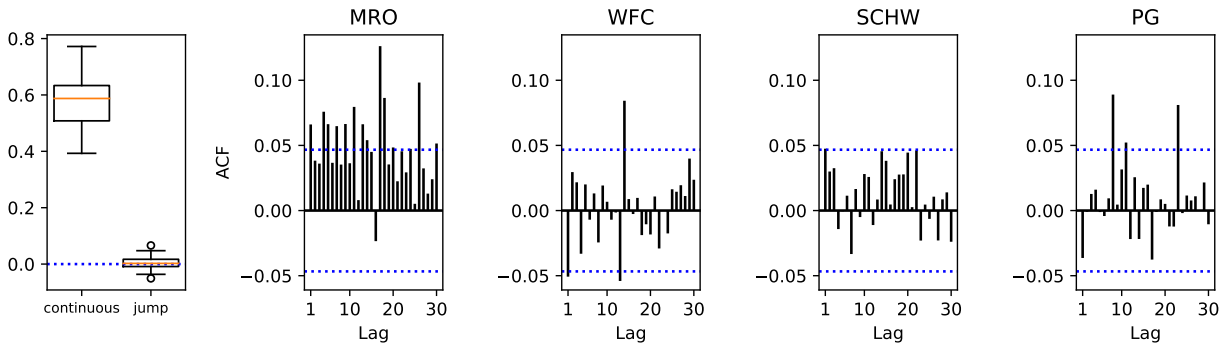

Figure 7: The box plot (left) of the first-order autocorrelations of RIB (continuous) and jump beta (jump) from January 1, 2010, to December 31, 2016, and the ACF plots for the top four first-order autocorrelation stocks.

500 index futures as the market portfolio, which was obtained from Refinitiv Tick History. We used 1-sec log-returns, which were subsampled by the previous tick (Zhang, 2011) scheme. High-frequency data were available between the open and close of the market, so the number of high-frequency observations for a full trading day is $m = 23400$.

To examine the goodness of fit, we conducted in-sample validation. We draw autocorrelation plots for RIB and jump beta in Figures 1 and 7, where the jump beta is estimated by the method suggested by Li et al. (2017b). As we discussed in Section 3, the integrated beta for the continuous part has a strong autocorrelation structure, but the beta for the jumps does not. Thus, it is reasonable to focus on modeling the beta for the continuous part. To conduct the validation of the DR Beta model, we first selected the $(p, q) \in \{(p, q) : 0 \leq p, q \leq 5\}$ of the DR Beta for each stock by BIC, and we estimated the parameters of the DR Beta using the sample over the last 1000 trading days. Then, we conducted the hypothesis tests proposed in Section 3.2.3. Table 1 reports the parameter estimates of the DR Beta model with the selected (p, q) for each stock and their p-values. The BIC values were minimized when $(p, q) = (1, 1)$ for all stocks. All coefficients are significant at a significance level of 0.05, except for the case of the AMD. On the other hand, the higher $\gamma_1^g + \alpha_1^g$ implies more persistent integrated beta process. From Table 1, we find that all stocks have the $\gamma_1^g + \alpha_1^g$ greater than 0.8, and for 36 stocks out of 50, $\gamma_1^g + \alpha_1^g$ is greater than 0.9. Thus, we can conclude that the proposed DR Beta model is statistically valid and may capture the persistent

Table 1: Estimated parameters from the DR Beta model. The numbers in parentheses indicate the p-value, multiplied by 10, from the hypothesis tests.

Stock	ω	γ_1^g	α_1^g	Stock	ω	γ_1^g	α_1^g
AAPL	0.126 (0.0)	0.539 (0.0)	0.325 (0.0)	JPM	0.076 (0.0)	0.608 (0.0)	0.314 (0.0)
AIG	0.063 (0.0)	0.623 (0.0)	0.308 (0.0)	KEY	0.111 (0.0)	0.542 (0.0)	0.354 (0.0)
AMAT	0.190 (0.0)	0.491 (0.0)	0.323 (0.0)	KO	0.030 (0.0)	0.653 (0.0)	0.288 (0.0)
AMD	0.011 (1.0)	0.826 (0.0)	0.163 (0.0)	MGM	0.045 (0.0)	0.715 (0.0)	0.248 (0.0)
ATVI	0.088 (0.0)	0.618 (0.0)	0.283 (0.0)	MRK	0.056 (0.0)	0.622 (0.0)	0.299 (0.0)
BAC	0.083 (0.0)	0.608 (0.0)	0.315 (0.0)	MRO	0.042 (0.0)	0.618 (0.0)	0.352 (0.0)
BMY	0.070 (0.0)	0.604 (0.0)	0.310 (0.0)	MS	0.117 (0.0)	0.547 (0.0)	0.359 (0.0)
BSX	0.121 (0.0)	0.540 (0.0)	0.330 (0.0)	MSFT	0.072 (0.0)	0.619 (0.0)	0.301 (0.0)
CSCO	0.112 (0.0)	0.541 (0.0)	0.326 (0.0)	MU	0.091 (0.0)	0.683 (0.0)	0.254 (0.0)
CSX	0.073 (0.0)	0.607 (0.0)	0.314 (0.0)	NEM	0.025 (0.0)	0.588 (0.0)	0.339 (0.0)
DAL	0.096 (0.0)	0.604 (0.0)	0.304 (0.0)	NFLX	0.047 (0.0)	0.720 (0.0)	0.246 (0.0)
DIS	0.071 (0.0)	0.619 (0.0)	0.293 (0.0)	NVDA	0.176 (0.0)	0.456 (0.0)	0.374 (0.0)
DOW	0.051 (0.0)	0.698 (0.0)	0.249 (0.0)	ORCL	0.111 (0.0)	0.540 (0.0)	0.326 (0.0)
EBAY	0.106 (0.0)	0.554 (0.0)	0.327 (0.0)	PFE	0.050 (0.0)	0.650 (0.0)	0.281 (0.0)
F	0.071 (0.0)	0.605 (0.0)	0.311 (0.0)	PG	0.030 (0.0)	0.653 (0.0)	0.288 (0.0)
FCX	0.031 (0.1)	0.675 (0.0)	0.303 (0.0)	QCOM	0.077 (0.0)	0.568 (0.0)	0.335 (0.0)
FITB	0.066 (0.0)	0.614 (0.0)	0.323 (0.0)	RF	0.070 (0.0)	0.652 (0.0)	0.286 (0.0)
GE	0.129 (0.0)	0.489 (0.0)	0.332 (0.0)	SCHW	0.112 (0.0)	0.554 (0.0)	0.355 (0.0)
GILD	0.070 (0.0)	0.607 (0.0)	0.327 (0.0)	T	0.026 (0.0)	0.706 (0.0)	0.240 (0.0)
GLW	0.142 (0.0)	0.564 (0.0)	0.287 (0.0)	VZ	0.027 (0.0)	0.707 (0.0)	0.241 (0.0)
HAL	0.067 (0.0)	0.644 (0.0)	0.296 (0.0)	WFC	0.111 (0.0)	0.540 (0.0)	0.326 (0.0)
HBAN	0.047 (0.0)	0.674 (0.0)	0.278 (0.0)	WMB	0.026 (0.1)	0.699 (0.0)	0.278 (0.0)
HPQ	0.178 (0.0)	0.526 (0.0)	0.301 (0.0)	WMT	0.038 (0.0)	0.625 (0.0)	0.298 (0.0)
HST	0.077 (0.0)	0.618 (0.0)	0.295 (0.0)	XOM	0.063 (0.0)	0.550 (0.0)	0.368 (0.0)
INTC	0.108 (0.0)	0.552 (0.0)	0.324 (0.0)	XRX	0.138 (0.0)	0.568 (0.0)	0.283 (0.0)

Table 2: The mean of RIB estimates in the out-of-sample period and the MAPEs for the DR Beta, ARMAC, ARMAP, PRBG, RBG, DCC, and BEKK for each stock.

Stock	RIB	DRBeta	ARMAC	ARMAP	PRBG	RBG	DCC	BEKK	Stock	RIB	DRBeta	ARMAC	ARMAP	PRBG	RBG	DCC	BEKK
AAPL	0.985	0.238	0.254	0.259	0.300	0.279	0.324	0.326	JPM	1.030	0.170	0.203	0.211	0.293	0.274	0.325	0.314
AIG	0.989	0.183	0.206	0.225	0.348	0.326	0.346	0.407	KEY	1.064	0.226	0.252	0.276	0.334	0.366	0.406	0.363
AMAT	1.028	0.215	0.235	0.262	0.388	0.397	0.443	0.365	KO	0.499	0.117	0.127	0.134	0.168	0.167	0.214	0.186
AMD	0.950	0.371	0.382	0.444	0.779	0.892	0.936	0.953	MGM	1.295	0.280	0.302	0.347	0.468	0.434	0.583	0.590
ATVI	0.847	0.208	0.225	0.242	0.313	0.331	0.359	0.293	MRK	0.674	0.142	0.162	0.159	0.341	0.185	0.241	0.218
BAC	1.181	0.240	0.261	0.303	0.431	0.382	0.465	0.490	MRO	1.400	0.295	0.325	0.349	0.404	0.412	0.562	0.595
BMY	0.740	0.163	0.185	0.184	0.248	0.237	0.312	0.271	MS	1.350	0.228	0.273	0.286	0.369	0.365	0.424	0.456
BSX	0.873	0.219	0.240	0.265	0.432	0.430	0.486	0.396	MSFT	0.889	0.168	0.191	0.194	0.260	0.269	0.293	0.223
CSCO	0.871	0.169	0.193	0.197	0.238	0.264	0.273	0.250	MU	1.444	0.329	0.363	0.379	0.531	0.525	0.653	0.593
CSX	0.943	0.180	0.205	0.224	0.302	0.282	0.404	0.385	NEM	0.466	0.277	0.279	0.286	0.407	0.452	0.535	0.514
DAL	1.016	0.263	0.280	0.305	0.626	0.422	0.511	0.431	NFLX	1.334	0.315	0.347	0.356	0.437	0.406	0.575	0.578
DIS	0.810	0.140	0.162	0.172	0.230	0.222	0.287	0.260	NVDA	1.104	0.237	0.256	0.283	0.376	0.374	0.496	0.460
DOW	0.995	0.186	0.206	0.232	0.343	0.311	0.405	0.478	ORCL	0.868	0.160	0.179	0.195	0.264	0.240	0.303	0.293
EBAY	0.936	0.185	0.207	0.212	0.300	0.279	0.360	0.307	PFE	0.700	0.149	0.166	0.170	0.188	0.204	0.235	0.199
F	0.903	0.206	0.212	0.262	0.377	0.388	0.483	0.438	PG	0.483	0.119	0.131	0.128	0.178	0.162	0.204	0.187
FCX	1.398	0.315	0.343	0.368	0.562	0.565	0.708	0.768	QCOM	0.845	0.157	0.181	0.179	0.250	0.238	0.349	0.273
FITB	1.046	0.199	0.229	0.254	0.290	0.299	0.346	0.346	RF	1.156	0.250	0.270	0.322	0.456	0.477	0.495	0.517
GE	0.769	0.151	0.164	0.190	0.241	0.264	0.321	0.298	SCHW	1.210	0.221	0.258	0.276	0.375	0.350	0.418	0.347
GILD	0.996	0.210	0.242	0.247	0.505	0.304	0.371	0.410	T	0.498	0.120	0.128	0.136	0.187	0.213	0.246	0.201
GLW	0.958	0.197	0.212	0.249	0.330	0.354	0.430	0.371	VZ	0.520	0.129	0.138	0.144	0.162	0.168	0.215	0.182
HAL	1.195	0.238	0.264	0.281	0.365	0.375	0.451	0.485	WFC	0.876	0.151	0.173	0.188	0.276	0.259	0.326	0.337
HBAN	0.957	0.218	0.236	0.286	0.471	0.509	0.475	0.483	WMB	1.073	0.257	0.277	0.301	0.351	0.336	0.553	0.568
HPQ	1.050	0.226	0.252	0.262	0.304	0.278	0.375	0.330	WMT	0.483	0.113	0.126	0.127	0.176	0.159	0.224	0.166
HST	0.923	0.198	0.211	0.245	0.404	0.411	0.530	0.514	XOM	0.778	0.136	0.159	0.163	0.191	0.190	0.226	0.217
INTC	0.895	0.163	0.186	0.197	0.228	0.257	0.297	0.246	XRX	0.919	0.235	0.242	0.289	0.509	0.537	0.566	0.447

autoregressive structure.

To evaluate the out-of-sample performance, we computed the mean absolute prediction error (MAPE) as follows:

$$\frac{1}{n-500}\sum_{i=501}^{n}\left|\widehat{Beta}_i - RIB_i\right|,$$

where $\widehat{Beta}_i$ denotes the one-day-ahead forecasted beta from parametric models such as DR Beta, ARMAC, ARMAP, PRBG, RBG, DCC, and BEKK, as defined in Section 4, using a sample size of 500 for in-sample data. Unlike in a simulation study where the true integrated beta is known, it is impossible to obtain the true integrated beta in the empirical study. Therefore, we need to use the proxy of the true integrated beta when calculating MAPE. Since, to the best of our knowledge, the proposed RIB estimator is the only consistent estimator of integrated beta, we employed the RIB estimator as the proxy of the true integrated beta. For each stock, we used the selected (p, q) order for the DR Beta, ARMAC, and ARMAP models. In the case of ARMAC, we also checked their performance with input integrated betas estimated by CHEN with data subsampled at 1, 5, 10, 30, and 60-second frequencies to deal with the autocorrelated microstructure noise. Then, we reported the best performance results among the different frequencies. For RBG, we used realized covariance, the sum of squared log-returns, with 5-min, 1-min, and 30-sec data ($m = 78, 390, 780$, respectively) to handle the microstructure noise, and reported the best results among them. The in-sample period is 500 days, and we estimated the models using the rolling window scheme. Table 2 reports the mean of RIB estimates in the out-of-sample period and the MAPEs for DR Beta, ARMAC, ARMAP, PRBG, RBG, DCC, and BEKK for 50 stocks. From Table 2, we find that the models using high-frequency information show better performance than the models using only low-frequency information. Further, the ARMA-type models utilizing realized betas usually perform better than the RBG and PRBG models. When comparing the ARMA-type models using realized betas, MAPEs for the proposed DR Beta or ARMAC have the smallest values for every stock, and DR Beta always shows the lowest MAPE among the benchmarks. It may be because the proposed DR Beta and ARMAC model can account for the time-varying beta by incorporating high-

frequency data. These results indicate that accommodating the time-varying beta feature helps account for the beta dynamics, and the DR Beta holds advantages in predicting future integrated beta by utilizing the autoregressive structure with consistent RIB estimates.

We evaluated how well the proposed methodologies capture the autoregressive structure. Adopting the idea of the Durbin-Watson test, we took into account regression residuals between the non-parametric and out-of-sample predicted values using DR Beta, ARMAC, ARMAP, PRBG, RBG, DCC, and BEKK. Specifically, for each model, we fitted the following linear regression model:

$$RIB_i = a + b \times \widehat{Beta}_i + e_i,$$

where the $\widehat{Beta}_i$'s are one-day-ahead forecasted betas obtained using one of the DR Beta, ARMAC, ARMAP, PRBG, RBG, DCC, and BEKK. Then, we calculated the regression residuals for each model and checked their autocorrelations.

Table 3 reports the first-order autocorrelations of the regression residuals for each model. For ARMAC, only the result of the case with the lowest first-order autocorrelations of the regression residuals among the different sample frequencies is reported for each stock. We further provide the ACF plots for RIB and the models' regression residuals (Figure A3) and the box plot of the first-order autocorrelations of the regression residuals for each model (Figure A4) in the online Appendix. From Table 3 and Figures A3 and A4, we find that the proposed DR Beta and ARMAC models have much smaller autocorrelations for most of the assets, but the other models still yield significantly non-zero autocorrelations for most of the assets. This may be because the other competitors could not appropriately estimate the integrated beta due to the time-varying beta feature. When comparing the DR Beta and ARMAC models, the DR Beta model usually has smaller autocorrelation than the ARMAC model. Specifically, for 28 stocks out of 50, DR Beta shows the best performance among the benchmarks. One of the possible explanations is that the CHEN estimator, which is used in the ARMAC model as the non-parametric beta estimator, cannot handle the autocorrelation structure of the microstructure noise; thus, some autocorrelation may remain in the regression residuals. From these numerical results, we can conjecture that incorporating the stylized features, such as the time-varying beta and the autocorrelation

Table 3: The first-order autocorrelations for the regression residuals between the non-parametric integrated beta estimates, RIB, and the predicted integrated beta from DR Beta, ARMAC, ARMAP, PRBG, RBG, DCC, and BEKK.

Stock	RIB	DRBeta	ARMAC	ARMAP	PRBG	RBG	DCC	BEKK	Stock	RIB	DRBeta	ARMAC	ARMAP	PRBG	RBG	DCC	BEKK
AAPL	0.583	0.048	0.095	0.173	0.259	0.292	0.512	0.571	JPM	0.548	0.036	0.045	0.262	0.319	0.319	0.497	0.513
AIG	0.620	0.056	0.054	0.217	0.241	0.232	0.485	0.472	KEY	0.554	0.062	0.079	0.264	0.335	0.412	0.552	0.556
AMAT	0.415	0.047	0.059	0.267	0.347	0.344	0.406	0.415	KO	0.598	0.050	0.061	0.206	0.309	0.348	0.598	0.598
AMD	0.578	0.052	0.070	0.124	0.331	0.456	0.517	0.571	MGM	0.584	0.086	0.065	0.276	0.386	0.297	0.583	0.570
ATVI	0.476	0.051	0.007	0.245	0.361	0.345	0.473	0.428	MRK	0.574	0.049	0.024	0.252	0.568	0.299	0.537	0.513
BAC	0.644	0.057	0.075	0.240	0.315	0.339	0.508	0.615	MRO	0.777	0.080	0.095	0.266	0.283	0.339	0.600	0.578
BMY	0.610	0.038	0.001	0.213	0.317	0.305	0.569	0.519	MS	0.628	0.085	0.076	0.280	0.331	0.330	0.507	0.623
BSX	0.498	0.063	0.068	0.237	0.459	0.461	0.476	0.487	MSFT	0.474	0.038	0.039	0.259	0.327	0.320	0.473	0.428
CSCO	0.466	0.061	0.079	0.255	0.340	0.392	0.466	0.457	MU	0.484	0.054	0.061	0.244	0.312	0.294	0.469	0.484
CSX	0.535	0.080	0.064	0.290	0.341	0.347	0.530	0.525	NEM	0.689	0.057	0.062	0.141	0.301	0.398	0.660	0.679
DAL	0.485	0.070	0.068	0.257	0.466	0.341	0.483	0.471	NFLX	0.544	0.032	0.036	0.213	0.327	0.321	0.542	0.543
DIS	0.472	0.040	0.021	0.272	0.345	0.337	0.470	0.465	NVDA	0.544	0.077	0.084	0.257	0.301	0.293	0.503	0.493
DOW	0.558	0.040	0.015	0.228	0.268	0.280	0.478	0.495	ORCL	0.503	0.046	0.028	0.239	0.351	0.274	0.478	0.481
EBAY	0.514	0.080	0.032	0.228	0.278	0.312	0.500	0.493	PFE	0.470	0.033	0.034	0.156	0.270	0.305	0.457	0.455
F	0.499	0.052	0.037	0.258	0.354	0.354	0.487	0.461	PG	0.615	0.043	0.061	0.196	0.378	0.322	0.597	0.609
FCX	0.753	0.026	0.049	0.220	0.164	0.256	0.494	0.549	QCOM	0.590	0.042	0.042	0.270	0.306	0.310	0.570	0.563
FITB	0.603	0.053	0.080	0.289	0.375	0.418	0.559	0.593	RF	0.571	0.064	0.092	0.270	0.448	0.456	0.556	0.570
GE	0.474	0.056	0.037	0.264	0.334	0.350	0.475	0.462	SCHW	0.508	0.040	0.045	0.269	0.371	0.315	0.508	0.503
GILD	0.661	0.094	0.071	0.306	0.632	0.343	0.610	0.643	T	0.470	0.040	0.034	0.207	0.354	0.379	0.470	0.470
GLW	0.391	0.034	0.047	0.222	0.338	0.345	0.359	0.383	VZ	0.480	0.077	0.069	0.224	0.301	0.330	0.480	0.479
HAL	0.616	0.066	0.066	0.269	0.346	0.338	0.587	0.593	WFC	0.579	0.076	0.081	0.285	0.376	0.358	0.515	0.524
HBAN	0.547	0.047	0.049	0.246	0.498	0.515	0.546	0.516	WMB	0.715	0.021	0.010	0.230	0.272	0.248	0.516	0.477
HPQ	0.454	0.077	0.052	0.270	0.316	0.309	0.447	0.445	WMT	0.514	0.051	0.061	0.198	0.379	0.353	0.514	0.513
HST	0.517	0.065	0.053	0.245	0.342	0.378	0.486	0.501	XOM	0.603	0.064	0.068	0.315	0.379	0.348	0.598	0.603
INTC	0.499	0.051	0.055	0.280	0.371	0.416	0.499	0.498	XRX	0.379	0.061	0.046	0.196	0.357	0.364	0.344	0.377

structure of the microstructure noise, helps account for the integrated beta dynamics. Thus, the proposed DR Beta model can explain the integrated beta dynamics well by incorporating the proposed robust realized integrated beta estimator.

Finally, to check the economic benefits of predicting future market beta, we analyzed the out-of-sample performance of the market-neutral portfolios. We considered the close-to-close log-returns of market-neutral portfolios constructed by holding a share of an asset, simultaneously taking a short position in E-mini S&P 500 index futures contracts. The amount of the futures contracts, namely the hedging ratio, was calibrated using the one-day-ahead forecasted beta as follows:

$$(\widehat{a}, \widehat{b}) = \text{argmin}_{a,b} \sum_{i=1}^{n} (R_{A,i} - (a + b\widetilde{h}_i) R_{M,i})^2,$$

where $(\widetilde{h}_i)_{i=1,\ldots,n}$ are in-sample fitted betas, and $R_{A,i}$ and $R_{M,i}$ are the ith close-to-close log-returns of an asset and the market portfolio, respectively. That is, the forecasted hedging ratio is $\widehat{a}+\widehat{b}\widehat{Beta}_{n+1}$. To evaluate the effectiveness of the hedging, we calculated the absolute correlation, the hedging effectiveness (Ederington, 1979), and the ex-post portfolio beta between the hedged portfolio and the market portfolio as follows:

$$\text{Absolute correlation} = \left| \frac{\text{cov}(R_H, R_M)}{\sqrt{\text{var}(R_H)\text{var}(R_H)}} \right|,$$
$$\text{Hedging effectiveness} = 1 - \frac{\text{var}(R_H)}{\text{var}(R_A)}, \quad \text{and} \quad \text{Ex-post beta} = \frac{\text{cov}(R_H, R_M)}{\text{var}(R_M)},$$

where $R_{H,i} = R_{A,i} - (\widehat{a}+\widehat{b}\widehat{Beta}_i) R_{M,i}$ denotes the hedged portfolio's out-of-sample log-return.

Table 4: The mean absolute correlation, hedging effectiveness, and ex-post beta between the hedged portfolios and the market portfolio, where the hedged portfolios are constructed based on the predicted beta using the OLS regression beta, DR Beta, ARMAC, ARMAP, PRBG, RBG, DCC, and BEKK. Unhedged indicates the unhedged single-asset portfolio.

Measure \ Model	Unhedged	OLS	DR Beta	ARMAC	ARMAP	PRBG	RBG	DCC	BEKK
Absolute Correlation	0.569	0.031	0.020	0.021	0.023	0.064	0.060	0.033	0.029
Hedging Effectiveness	0.000	0.334	0.338	0.337	0.339	0.330	0.331	0.333	0.330
Ex-post beta	1.154	0.057	0.034	0.035	0.038	0.124	0.115	0.058	0.054

Table 4 reports the mean of absolute correlation, hedging effectiveness, and ex-post beta for the unhedged single-asset portfolio (Unhedged), hedged portfolio using the one-day-ahead forecasted beta from the regression beta (OLS), DR Beta, ARMAC, ARMAP, PRBG, RBG, DCC, and BEKK models. For the forecasted beta using OLS, we employed the beta derived from OLS regression on daily close-to-close log-returns, using a sample size of 500 in-samples. From Table 4, we find that the ARMA models incorporating high-frequency-based non-parametric estimators as inputs show the best performance in hedging the market factor. While the ARMA models provided comparable performances, incorporating the RIB estimator led to an improvement in the absolute correlation and ex-post beta measures. In the case of hedging effectiveness, the ARMAP is slightly better than the DR Beta model.

6 Conclusion

This paper investigates integrated market betas based on high-frequency financial data. We first develop a robust non-parametric integrated beta estimation procedure, RIB, which can handle the price-dependent and autocorrelated microstructure noise and time-varying beta. Then, we establish its asymptotic properties. With this robust non-parametric RIB estimator, we find the time-series structure of the integrated betas. To account for this beta dynamics, we propose the DR Beta model. To estimate the model parameters, we propose a quasi-likelihood estimation procedure and establish its asymptotic theorems. From the empirical study, we find that the proposed DR Beta model using the robust realized integrated beta estimator helps account for the integrated beta dynamics.

Acknowledgment

The authors thank the co-Editor Professor Torben Andersen, and anonymous associate editor and two referees for their careful reading of this paper and valuable comments. The research of Donggyu Kim was supported by KAIST Basic Research Funds by Faculty (A0601003029) and the National Research Foundation of Korea (NRF) (2021R1C1C1003216).

References

Adrian, T. and Franzoni, F. (2009). Learning about beta: Time-varying factor loadings, expected returns, and the conditional capm. *Journal of Empirical Finance*, 16(4):537–556.

Aït-Sahalia, Y., Fan, J., and Xiu, D. (2010). High-frequency covariance estimates with noisy and asynchronous financial data. *Journal of the American Statistical Association*, 105(492):1504–1517.

Aït-Sahalia, Y. and Jacod, J. (2009). Estimating the degree of activity of jumps in high frequency data. *The Annals of Statistics*, 37(5A):2202–2244.

Aït-Sahalia, Y., Kalnina, I., and Xiu, D. (2020). High-frequency factor models and regressions. *Journal of Econometrics*.

Aït-Sahalia, Y., Mykland, P. A., and Zhang, L. (2011). Ultra high frequency volatility estimation with dependent microstructure noise. *Journal of Econometrics*, 160(1):160–175.

Aït-Sahalia, Y. and Xiu, D. (2016). Increased correlation among asset classes: Are volatility or jumps to blame, or both? *Journal of Econometrics*, 194(2):205–219.

Aït-Sahalia, Y. and Yu, J. (2009). High frequency market microstructure noise estimates and liquidity measures. *The Annals of Applied Statistics*, 3(1):422 – 457.

Andersen, T. G., Bollerslev, T., Diebold, F. X., and Wu, G. (2006). *Realized Beta: Persistence and Predictability*, volume 20 Part 2 of *Advances in Econometrics*. Emerald Group Publishing Limited.

Andersen, T. G., Thyrsgaard, M., and Todorov, V. (2021). Recalcitrant betas: Intraday variation in the cross-sectional dispersion of systematic risk. *Quantitative Economics*, 12(2):647–682.

Ang, A. and Chen, J. (2007). CAPM over the long run: 1926–2001. *Journal of Empirical Finance*, 14(1):1–40.

Bali, T. G. and Engle, R. F. (2010). The intertemporal capital asset pricing model with dynamic conditional correlations. *Journal of Monetary Economics*, 57(4):377–390.

Barndorff-Nielsen, O. E., Hansen, P. R., Lunde, A., and Shephard, N. (2008). Designing realized kernels to measure the ex post variation of equity prices in the presence of noise. *Econometrica*, 76(6):1481–1536.

Barndorff-Nielsen, O. E., Hansen, P. R., Lunde, A., and Shephard, N. (2011). Multivariate realised kernels: consistent positive semi-definite estimators of the covariation of equity prices with noise and non-synchronous trading. *Journal of Econometrics*, 162(2):149–169.

Barndorff-Nielsen, O. E. and Shephard, N. (2004). Econometric analysis of realized covariation: High frequency based covariance, regression, and correlation in financial economics. *Econometrica*, 72(3):885–925.

Becker, J., Hollstein, F., Prokopczuk, M., and Sibbertsen, P. (2021). The memory of beta. *Journal of Banking & Finance*, 124:106026.

Black, A., Fraser, P., and Power, D. (1992). UK unit trust performance 1980–1989: A passive time-varying approach. *Journal of Banking & Finance*, 16(5):1015–1033.

Blume, M. E. (1971). On the assessment of risk. *The Journal of Finance*, 26(1):1–10.

Bollerslev, T., Li, S. Z., and Todorov, V. (2016). Roughing up beta: Continuous versus discontinuous betas and the cross section of expected stock returns. *Journal of Financial Economics*, 120(3):464–490.

Bos, T. and Newbold, P. (1984). An empirical investigation of the possibility of stochastic systematic risk in the market model. *Journal of Business*, pages 35–41.

Breen, W., Glosten, L. R., and Jagannathan, R. (1989). Economic significance of predictable variations in stock index returns. *The Journal of Finance*, 44(5):1177–1189.

Chen, R. Y. (2018). Inference for volatility functionals of multivariate Itô semimartingales observed with jump and noise. *arXiv preprint arXiv:1810.04725*.

Christensen, K., Kinnebrock, S., and Podolskij, M. (2010). Pre-averaging estimators of the ex-post covariance matrix in noisy diffusion models with non-synchronous data. *Journal of Econometrics*, 159(1):116–133.

Ederington, L. H. (1979). The hedging performance of the new futures markets. *The Journal of Finance*, 34(1):157–170.

Engle, R. F. (2016). Dynamic conditional beta. *Journal of Financial Econometrics*, 14(4):643–667.

Engle, R. F. and Kroner, K. F. (1995). Multivariate simultaneous generalized ARCH. *Econometric Theory*, pages 122–150.

Fama, E. F. and French, K. R. (2004). The capital asset pricing model: Theory and evidence. *Journal of Economic Perspectives*, 18(3):25–46.

Fama, E. F. and MacBeth, J. D. (1973). Risk, return, and equilibrium: Empirical tests. *Journal of Political Economy*, 81(3):607–636.

Fan, J. and Kim, D. (2018). Robust high-dimensional volatility matrix estimation for high-frequency factor model. *Journal of the American Statistical Association*, 113(523):1268–1283.

Figueroa-López, J. E. and Wu, B. (2022). Kernel estimation of spot volatility with microstructure noise using pre-averaging. *Econometric Theory*, pages 1–50.

González-Rivera, G. (1996). Time-varying risk the case of the american computer industry. *Journal of Empirical Finance*, 2(4):333–342.

Hansen, L. P. and Richard, S. F. (1987). The role of conditioning information in deducing testable restrictions implied by dynamic asset pricing models. *Econometrica: Journal of the Econometric Society*, pages 587–613.

Hansen, P. R. and Lunde, A. (2006). Realized variance and market microstructure noise. *Journal of Business & Economic Statistics*, 24(2):127–161.

Hansen, P. R., Lunde, A., and Voev, V. (2014). Realized beta GARCH: A multivariate GARCH model with realized measures of volatility. *Journal of Applied Econometrics*, 29(5):774–799.

Hautsch, N. and Podolskij, M. (2013). Preaveraging-based estimation of quadratic variation in the presence of noise and jumps: theory, implementation, and empirical evidence. *Journal of Business & Economic Statistics*, 31(2):165–183.

Hollstein, F. and Prokopczuk, M. (2016). Estimating beta. *Journal of Financial and Quantitative Analysis*, 51(4):1437–1466.

Jacod, J., Li, Y., Mykland, P. A., Podolskij, M., and Vetter, M. (2009). Microstructure noise in the continuous case: the pre-averaging approach. *Stochastic Processes and their Applications*, 119(7):2249–2276.

Jacod, J., Li, Y., and Zheng, X. (2017). Statistical properties of microstructure noise. *Econometrica*, 85(4):1133–1174.

Jacod, J., Li, Y., and Zheng, X. (2019). Estimating the integrated volatility with tick observations. *Journal of Econometrics*, 208(1):80–100.

Jacod, J. and Rosenbaum, M. (2013). Quarticity and other functionals of volatility: Efficient estimation. *The Annals of Statistics*, 41(3):1462 – 1484.

Keim, D. B. and Stambaugh, R. F. (1986). Predicting returns in the stock and bond markets. *Journal of Financial Economics*, 17(2):357–390.

Kim, D. and Wang, Y. (2016). Unified discrete-time and continuous-time models and statistical inferences for merged low-frequency and high-frequency financial data. *Journal of Econometrics*, 194(2):220–230.

Koreisha, S. G. and Fang, Y. (1999). The impact of measurement errors on ARMA prediction. *Journal of Forecasting*, 18(2):95–109.

Koutmos, G., Lee, U., and Theodossiu, P. (1994). Time-varying betas and volatility persistence in international stock markets. *Journal of Economics and Business*, 46(2):101–112.

Li, J., Todorov, V., and Tauchen, G. (2017a). Adaptive estimation of continuous-time regression models using high-frequency data. *Journal of Econometrics*, 200(1):36–47.

Li, J., Todorov, V., and Tauchen, G. (2017b). Robust jump regressions. *Journal of the American Statistical Association*, 112(517):332–341.

Li, J. and Xiu, D. (2016). Generalized method of integrated moments for high-frequency data. *Econometrica*, 84(4):1613–1633.

Li, Z. M., Laeven, R. J., and Vellekoop, M. H. (2020). Dependent microstructure noise and integrated volatility estimation from high-frequency data. *Journal of Econometrics*, 215(2):536–558.

Li, Z. M. and Linton, O. (2022). A ReMeDI for microstructure noise. *Econometrica*, 90(1):367–389.

Li, Z. M. and Linton, O. (2023). Robust estimation of integrated and spot volatility. *Journal of Econometrics*, page 105614.

Mykland, P. A. and Zhang, L. (2006). ANOVA for diffusions and Itô processes. *The Annals of Statistics*, 34(4):1931 – 1963.

Mykland, P. A. and Zhang, L. (2009). Inference for continuous semimartingales observed at high frequency. *Econometrica*, 77(5):1403–1445.

Ng, L. (1991). Tests of the CAPM with time-varying covariances: A multivariate GARCH approach. *The Journal of Finance*, 46(4):1507–1521.

Perold, A. F. (2004). The capital asset pricing model. *Journal of Economic Perspectives*, 18(3):3–24.

Reiß, M., Todorov, V., and Tauchen, G. (2015). Nonparametric test for a constant beta between Itô semi-martingales based on high-frequency data. *Stochastic Processes and their Applications*, 125(8):2955–2988.

Shin, M., Kim, D., and Fan, J. (2023). Adaptive robust large volatility matrix estimation based on high-frequency financial data. *Journal of Econometrics*, 237(1):105514.

Song, X., Kim, D., Yuan, H., Cui, X., Lu, Z., Zhou, Y., and Wang, Y. (2021). Volatility analysis with realized GARCH-Itô models. *Journal of Econometrics*, 222(1):393–410.

Ubukata, M. and Oya, K. (2009). Estimation and testing for dependence in market microstructure noise. *Journal of Financial Econometrics*, 7(2):106–151.

Xiu, D. (2010). Quasi-maximum likelihood estimation of volatility with high frequency data. *Journal of Econometrics*, 159(1):235–250.

Zhang, L. (2006). Efficient estimation of stochastic volatility using noisy observations: A multi-scale approach. *Bernoulli*, 12(6):1019–1043.

Zhang, L. (2011). Estimating covariation: Epps effect, microstructure noise. *Journal of Econometrics*, 160(1):33–47.

Zhang, L., Mykland, P. A., and Aït-Sahalia, Y. (2005). A tale of two time scales: Determining integrated volatility with noisy high-frequency data. *Journal of the American Statistical Association*, 100(472):1394–1411.

Zhang, X., Kim, D., and Wang, Y. (2016). Jump variation estimation with noisy high frequency financial data via wavelets. *Econometrics*, 4(3):34.